Franz Herbert Pirolt, BSc

Light Scattering in turbid and nonergodic systems

Exploring the possibilities of Multispeckle / Brute Force and 3D Echo DLS

MASTER'S THESIS

to achieve the university degree of

Master of Science

Master's degree programme: Chemistry

submitted to

Graz University of Technology

Suprevisor

Univ.-Prof.i.R. Dipl.-Ing. Dr.techn. Otto Glatter

Institut für Chemische Technologie von Materialien

Graz,December, 2014

EIDESSTATTLICHE ERKLÄRUNG

Ich erkläre an Eides statt, dass ich die vorliegende Arbeit selbstständig verfasst, andere als die angegebenen Quellen/Hilfsmittel nicht benutzt, und die den benutzten Quellen wörtlich und inhaltlich entnommenen Stellen als solche kenntlich gemacht habe. Das in TUGRAZonline hochgeladene Textdokument ist mit der vorliegenden Masterarbeit identisch.

AFFIDAVIT

I declare that I have authored this thesis independently, that I have not used other than the declared sources/resources, and that I have explicitly indicated all material which has been quoted either literally or by content from the sources used. The text document uploaded to TUGRAZonline is identical to the present master's thesis.

_____	_____
Datum / Date	Unterschrift / Signature

Acknowledgement

First I want to thank my boss and commandante Dr. Otto Glatter, for all his help in all imaginable forms. Be it advice for the experiments, financial support, infinite patcience or help in fighting bureau**cracy, THANK YOU**!

Furthermore I want to thank my dear colleagues Dr. Guillermo Ramon Iglesias for introducing me to these exciting methods, Dr. Amin Sadeghpour and Dr. Angela Chemelli for their relentless support in finishing this work, and constant helpful advice. I couldn't have done it without you!

Also I want to thank Günther Scherf for introducing me to the SAXSess and his guidance during numerous measurements.

A very special thank goes to my office colleague and Dr. to be Manuel Hollauf, for uncounted coffeebreaks and the constructive discussions that went along with them and MSc to be Tobias Müller for his scientific and culinaric support.

Finally I want to thank my parents, sisters and dearest friends, for their patience when I was ranting and grouching about something. I love you all!

Table of Contents

Preamble

This work is based on the preceding work of Dr. Norbert Freiberger and a previous post-doc project executed by Dr. Guillermo Ramon Iglesias. It includes a presentation of Dr. Iglesias's findings and a continuation of the research in this matter.

Abstract

English

This work examines the possibility to characterize turbid and nonergodic samples with two modified Dynamic Light Scattering techniques: 3D Echo DLS and Multispeckle. Both techniques are designed to obtain the long term dynamics of a colloidal system. To obtain the short term dynamics each method was combined with the Brute Force method.

A well-defined oil in water (O/W) emulsion comprised of liquid crystals (ISAsomes) was used to characterize the limitations of both methods in terms of turbidity. The same system was embedded in a hydrogel to test the applicability of the methods to investigate systems in different states of ergodicity. The size and structure of the used ISAsomes were checked by standard DLS and SAXS experiments.

3D Echo DLS is a good solution to measure the dynamics in a system that shows low turbidity on a time scale of up to 10^4 s. For higher concentrations of ISAsomes ($\geq$ 1.5w%) multiple scattering predominates the signal and not enough single scattered light reaches the photomultipliers to give a sufficient signal.

The Multispeckle method is applicable for higher concentrations of ISAsomes (10w% and higher) but at lower concentrations the signal strength decreases, so it is no longer possible to measure a correlation function. However this method does not eliminate multiple scattering. Dynamical information can be obtained on a time scale of up to 10^5 s.

Deutsch

Diese Arbeit untersucht die Möglichkeit trübe und nicht ergodische Proben mit zwei modifizierten dynamischen Lichtstreumethoden zu untersuchen: 3D Echo DLS und Multispeckle. Beide Methoden wurden entwickelt um die Langzeitdynamik von kolloidalen Systemen zu erfassen. Jede der beiden Methoden wurde zusätzlich mit der Brute Force Methode kombiniert um Informationen über Kurzzeitdynamik zu erhalten.

Eine genau definierte Öl in Wasser (O/W) Emulsion, bestehend aus Flüssigkristallen (ISAsomes) wurde benutzt um die Grenzen beider Methoden in Bezug auf Trübheit zu überprüfen. Dasselbe System der ISAsomen wurde in ein Hydrogel eingeschlossen um die Anwendbarkeit der Methoden auf Systeme in unterschiedlichen Ergodizitätszuständen zu testen. Die Größe und Struktur der verwendeten ISAsomen wurde mit Standard DLS und SAXS Experimenten überprüft.

3D Echo DLS bietet eine gute Möglichkeit die Dynamik in einem System, das eine geringe Trübung aufweist auf einer Zeitskala von bis zu 10^4 s zu messen. Bei höheren Konzentrationen an ISAsomen (≥ 1.5w%) überwiegt der Anteil an Mehrfachstreuung und nicht genug einfach gestreutes Licht erreicht die Photomultiplier um ein auswertbares Signal zu geben.

Die Multispeckle Methode ist anwendbar für höhere Konzentrationen von ISAsomen (10w% und höher). Diese Methode eliminiert aber nicht die Mehrfachstreuung. Bei niedrigeren Konzentrationen ist die Signalstärke zu schwach, um eine Korrelationsfunktion zu messen. Dynamische Informationen können damit auf einer Zeitskala von bis zu 10^5 s erhalten werden.

Introduction

This work was conducted at the Karl-Franzens University in Graz, Department of Chemistry, Group of Prof. Dr. Otto Glatter.

Colloidal systems and related phenomena are a big part of various products in our society. Already thousands of years ago people used such phenomena for the production of cheese, the extraction of paste from bones, or the production of ink. Nowadays the examples are nearly endless. To name a few: pharmaceutical and cosmetic products, dyes and paints, products in food industry, chemicals in agriculture.[1]

Another form of a colloidal system is an emulsion. An emulsion is a metastable system that is produced by mixing two immiscible fluids in the presence of a stabilizing agent (surface active substance) with some energy input. Through the Brownian motion the dispersed droplets are moving through the solution. According to their properties (size distribution, charge and surface activity) there will be some interactions between them leading to reversible or irreversible transitions. All irreversible transitions lead to coalescence and eventually phase separation and therefore the destruction of the emulsion. The simplest case of such a system is any kind of oil, stabilized in a continuous water phase with the help of a surfactant (hydrophilic head, lipophilic tail). The best known emulsion in nature is milk, where the proteins act as the surfactants. Due to the Bancroft rule[2,3] depending on the solubility properties of the surfactant a water in oil (w/o, surfactant is lipophilic) or an oil in water (o/w, surfactant is hydrophilic) emulsion is produced. According to this rule the surfactants are characterized by HLB numbers (Hydrophilic Lipophilic Balance) from 0 (very oil soluble) to 20 (very water soluble)[4].

In a further step it is possible to produce o/w emulsions that are internally nanostructured. This means that there is a liquid crystalline phase or a water in oil microemulsion that is stabilized in the continuous water phase. The internal structure of these emulsions can be tuned by the different oils that are used and by changing the temperature. Depending on the structure they are characterized as cubosomes (bicontinuous cubic), hexosomes (inverse hexagonal), micellar cubosomes (discontinuous inverse micellar cubic) and emulsified microemulsion.[5] The general

term for these structures that prevailed in the scientific community is ISAsomes (Internally Self Assembled particles or -somes). Hence different structures with numerous closed compartments can be produced. This is important to be able to incorporate hydrophilic as well as lipophilic and amphiphilic molecules. It has already been shown that it is possible to incorporate different substances, for example pesticides[6,7], pharmaceuticals[8], or different proteins[9] in such systems. With these properties nanostructured emulsions have the ability to pose as vehicles for active molecules and to ensure controlled delivery and sustained release.

A peculiar characteristic of these systems is that if two structures with different compositions are mixed they equilibrate and eventually will undergo a phase transition[10]. Current research investigates the possibility to use this behavior as micro-laboratories, to carry out sensitive or highly exothermic reactions under controlled conditions.

It is clear that the stability of the emulsions is of great importance for their applicability. Especially the average size and the size distribution of the droplets have a major influence on the stability and the behavior of the system[11]. Hence it is important to be able to measure these parameters of such systems.

Dynamic Light Scattering (DLS) is a well-known technique to study size, size distribution, interactions, and to some degree the shape of particles and soft matter systems. This can be done in the range from nanometers up to several micrometers. For a classical DLS experiment the sample has to be ergodic and transparent in order to gain the time average and therefore the ensemble average. It is abundantly clear that the above mentioned emulsions and also numerous industrial products are very often turbid, highly viscous, and in several cases even solid.

Colloidal dispersions (soft and hard matter), are in most cases turbid. This is caused by multiple scattering of the particles. It is clear that for the industrial use such systems are not produced in a highly diluted form, but as concentrated as necessary. Furthermore it is much more interesting to measure the original, untreated product, not least because the dynamics of a system are dependent on the concentration. This multiple scattering of the sample makes it hard or even impossible to measure the single scattering and evaluate the particle size or the dynamics.

In solid and even highly viscous products the movement of the particles is very slow or stopped (fixed). It is no longer possible to "see" all possible configurations of the particles (ensemble average) from a single, time averaged experiment.

To solve these problems several methods have been developed over the last decades. Examples are the 3D cross correlation[12], two-color light scattering[13] and diffusive wave spectroscopy (DWS)[14] to eliminate, or concerning the latter, even use multiple scattering from very turbid systems. The Brute force method, the Echo technique and the Multispeckle technique have been developed to deal with the problem of jellylike to solid (nonergodic) systems. By moving the sample and therefore shifting the scattering volume it is possible to collect enough measurements to gain the ensemble average for the short term dynamics. The Echo technique and the Multispeckle technique are used to obtain information about the long term dynamics. The use of very thin sample cells can help to reduce multiple scattering significantly. More detailed descriptions of these techniques can be found in the Theory chapter.

This work investigates a combination of these methods.

History

Scattered light is a constant part of our life. Most of the light that reaches our eyes is indirect light. The sky is blue because blue light is scattered more strongly in the atmosphere than higher wavelengths (red). The colors we see are determined by the absorption and scattering properties of the material.

Scattering methods are used for more than 100 years. The first scientist to conduct an experiment with visible light was John Tyndall in 1869. He filled a glass tube with different gases and observed their reaction and behavior upon their illumination with a light beam. [15]

It was only a few years later that Lord Rayleigh, a theoretician and experimentalist, could explain correctly why the sky is blue (1871). Furthermore he formulated the basics for Static Light Scattering (SLS) by explaining the scattering of spherical particles smaller than the wavelength of light. Later Debye and Gans contributed to this work by extending the theory to non-spherical particles (Rayleigh-Debye-Gans Theory, RDG). However this theory is limited to systems with a relative refractive index close to one. Eventually Ludvig Lorenz in 1890 and Gustav Mie in 1908 independently calculated the scattering of spheres of arbitrary size and refractive index. Gustav Mie also explained the scattering of particles bigger than the wavelength of light thus completing the range of spherical particles of any size. [16,17]

The biggest advance, to today's state of the art methods started with the invention of the LASER (Light Amplification by Stimulated Emission of Radiation) in the 60's. After the pioneer work of Max Planck in 1900, leading to the understanding of light as a form of electromagnetic radiation, it was Theodore Maiman in 1960 who invented the first working Laser. [18] Today the lasers that are used are generating collimated, monochromatic, coherent light with high power.

Theory

Scattering is always the result of heterogeneities of the system. The only perfectly homogeneous system is the vacuum. All other media possess inhomogeneities and hence scatter and absorb radiation.

Figure 1 shows what happens to an electromagnetic wave with Intensity (I_i), frequency (v_i), wavelength (λ_i) and polarization (P_i) when it passes through a particle of arbitrary shape. One part of the radiation is absorbed (I_{abs}), and another part of the radiation will be scattered. In this case of course we excluded the resonance phenomena and complete absorption.[19]
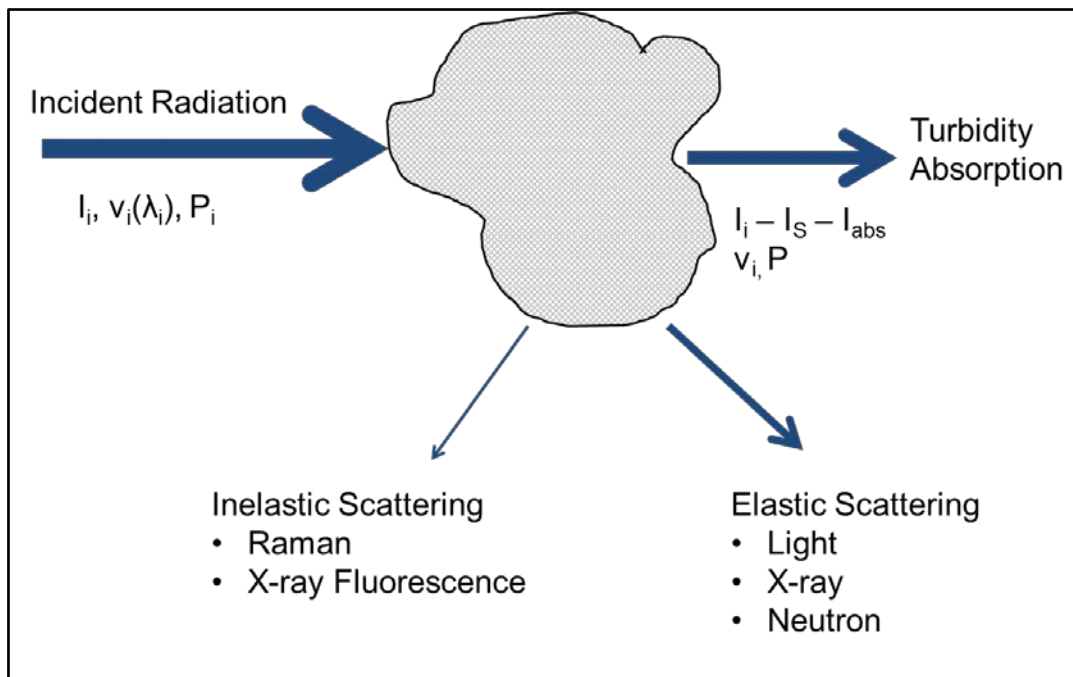
Figure 1: Interaction of an electromagnetic wave with matter [19]

Light causes a dipole oscillation of the outer electrons against the nuclei depending on the polarisability of the molecules. Dipole oscillation is equivalent to accelerated charge. This acceleration leads to the emission of a secondary "scattered" wave.

**Note: All variables in the equations printed bold are vectors!**

Interference

Usually we assume weak scattering, which means that most of the primary beam can pass through the sample without deviation and multiple scattering is negligible.

Furthermore elastic scattering is assumed, meaning that the frequency of the light is unchanged, and no energy transfer to the sample occurs.

In the case of two spatially separated scatterers, the pathlength of the scattered beams to the detector is different. This is described as the phase difference (φ).

The path length difference is derived from the different paths a and b (Figure 2).
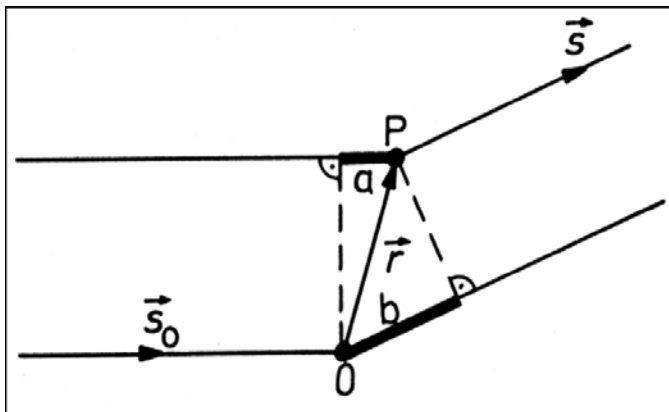
$$a = r\,s_0$$
$$b = r\,s$$
$$a - b = r\,s_0 - r\,s = -r\,(s - s_0)$$

The phase difference is calculated by multiplying the wave number with the path length difference.

$$\varphi = -\left(\frac{2\pi}{\lambda}\right) r(s - s_0)$$

Figure 2: Path difference of two beams

Scattering vector (q)

To express scattering data independent of the geometry of the experiment and independent of the wavelength (λ), the scattering vector $\boldsymbol{q}$ and its magnitude q is used (Figure 3)
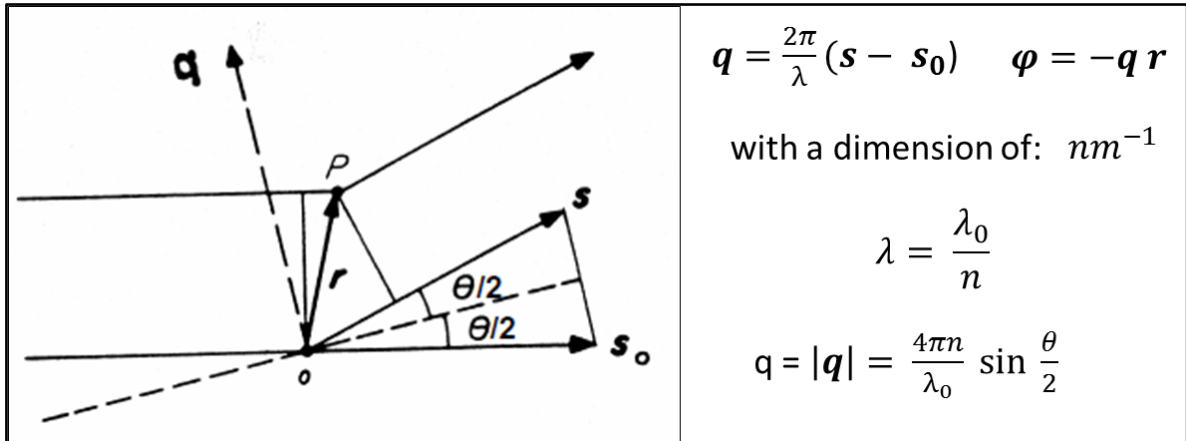

The equations shown in the figure:

$$q = \frac{2\pi}{\lambda}(s - s_0) \qquad \varphi = -q\,r$$

with a dimension of: nm^{-1}

$$\lambda = \frac{\lambda_0}{n}$$

$$q = |q| = \frac{4\pi n}{\lambda_0}\sin\frac{\theta}{2}$$

Figure 3: The scattering vector (q), which is perpendicular to the half scattering angle (θ/2); λ_0 is the wavelength in the vacuum; n is the refractive index, which is in case of x-rays and neutrons 1, hence λ is the wavelength in the medium.

This expresses the scattering of single atoms. Since in reality systems have more than one or a few atoms, the scattering length density (for neutrons), the electron density (for x-rays) and the refractive index (proportional to the polarisability of the atoms, for light) is introduced.

The scattering length density can be written as the sum of the mean density ($\bar{\rho}$) and its fluctuations ($\Delta\rho$)

$$\rho(\boldsymbol{r}) = \bar{\rho} + \Delta\rho(\boldsymbol{r}) \tag{Eq.1}$$

To get the total scattered field (E($\boldsymbol{q}$)) we have to integrate over the whole scattering volume. However, since the scattering volume normally is huge compared to the size of the scatterers of interest, the scattering from the mean density results in a peak at very low q-values and vanishes in the primary beam.

The total amplitude (E(**q**)) of an individual scatterer in the illuminated volume is found by summing up all scattering amplitudes, generated inside the particle, with their according phase.

Leaving us with the fluctuation (Δρ) we get:

$$E(\boldsymbol{q}) = \int_{V_{Particle}} \Delta\rho(\boldsymbol{r})e^{-i\boldsymbol{q}\boldsymbol{r}}\,d\boldsymbol{r} \qquad \text{(Eq.2)}$$

with e$^{-i\boldsymbol{q}\boldsymbol{r}}$ as the phase factor.

Since it is not possible to measure the total scattering amplitude, because the frequency of the oscillation of radiation is between 10^{15} (light) − 10^{18} (x-ray) and therefore technically not accessible, we measure the intensity (I(**q**)), which is the complex square of E(**q**):

$$I(\boldsymbol{q}) = E^{*}(\boldsymbol{q})E(\boldsymbol{q}) = \int_{V_{Particle}} \Delta\tilde{\rho}^{2}(\boldsymbol{r})e^{-i\boldsymbol{q}\boldsymbol{r}}\,d\boldsymbol{r} \qquad \text{(Eq.3)}$$

where $\Delta\tilde{\rho}^{2}$ is the convolution square of the scattering length density difference.

This leads to the phase problem, which means that it is not possible to determine the sign of the scattering length difference from the scattering pattern, but only the magnitude.

An important point of soft condensed materials is the movement of the particles due to the Brownian motion, in contrast to the fixed scattering centers in crystallography. Hence the scattering pattern of such systems is smeared, showing an average over all orientations in static experiments. The same situation is found for isotropic, noncrystalline materials. There defects or pores will not have a preferred orientation. Because of the phase problem and the averaging over all orientations it is impossible to derive the 3D structure of a particle in real space from its 1D scattering curve, while it is no problem in the reverse case.

There are several approaches to solve the inverse scattering problem. One is **Model Fitting** where a structure is assumed and its scattering curve is calculated. By varying the parameters of the model, the curve can be fitted to the scattering curve of

the measured sample. A disadvantage is that it is difficult to find a clear way of how to optimize the parameters. In the worst case the model is wrong but nevertheless gives a reasonable fit which leads to wrong results. The benefit is, once a good model is found, it is possible to get quantitative information about the structure.

Another possibility is to transform the scattering data into real space:

$$p(r) = \frac{1}{2\pi^2} \int_0^\infty I(q) \, qr \, \sin(qr) \, dr \qquad \text{(Eq.4)}$$

p(r) is also called the pair distance distribution function (PDDF) which is a histogram of all existing intra-particle distances multiplied with the scattering contrast differences at the end points.

In the case of a monodisperse homogeneous system the PDDF gives direct information about the shape of the particles. It is also possible to obtain information about the internal structure and the dimensions, for inhomogeneous systems.

However the direct transformation from the scattering function to the PDDF with Eq.4 is very often impossible, because of the experimental smearing effects and the fact that the scattering data is not available in the whole range of $0 \leq q \leq \infty$ (termination effect).

The solution of these problems is the **Indirect Fourier Transformation** (IFT) which is a model-free transformation of the scattering curve into the real space, depicted in Figure 4. This method uses only the transformation from real space to reciprocal space given in Eq.5.

$$I(q) = 4\pi \int_0^\infty p(r) \, \frac{\sin(qr)}{qr} \, dr \qquad \text{(Eq.5)}$$
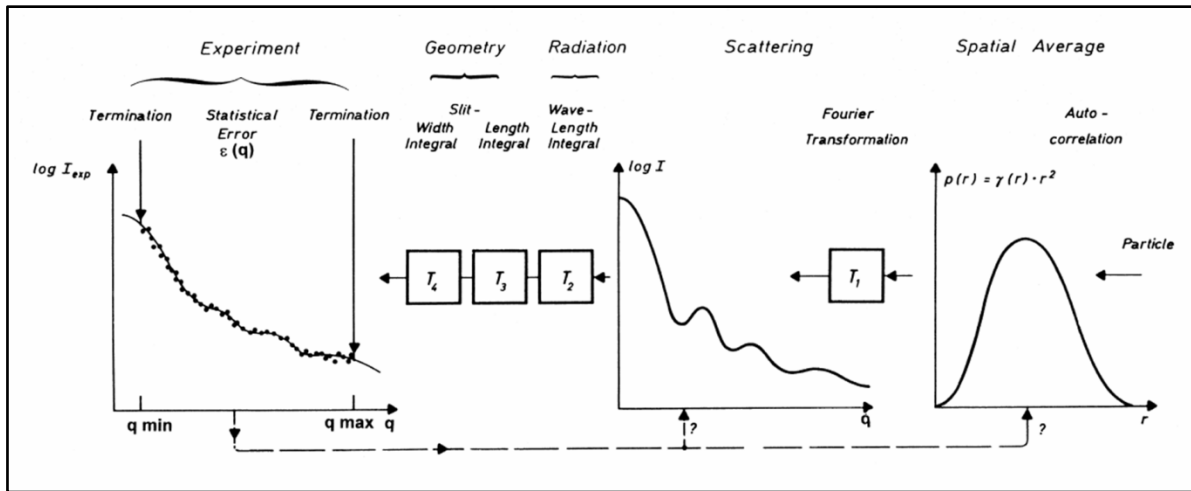
Figure 4: Schematic transformation between the PDDF (right side) to the scattering function[20]

The IFT solves the problem of the Fourier inversion simultaneously with the correction of the smearing effects.

To use the IFT method two things have to be known. One is that there is a finite particle dimension which matches the largest intra-particle distance (D_{max}), while if r > D_{max} the PDDF equals zero.

The second one is that the PDDF is representable with a sum of cubic B-splines ($\varphi_i(r)$) leading to a function with optimal smoothness (minimized second derivative).

$$p(r) = \sum_{i=1}^{n} c_i \varphi_i(r) \qquad \text{(Eq.6)}$$

The transformations T_1 (transformation from real to the reciprocal space) and T_2 to T_4 (taking care of the instrumental broadening) leaves us with three different sets of functions (φ, ψ, χ) but the same coefficients c_i (expansion coefficients) due to the linearity of these transformations. The scattering curve can now be fitted by calculating the expansion coefficients with a weighted least squares operation taking into account the standard deviation of the experimental data. With these coefficients c_i not only a fit to the data is found but also a desmeared curve and the corresponding PDDF.

Generalized Indirect Fourier Transformation (GIFT)

The IFT method is only valid for dilute systems, meaning there are no interactions between the particles. For globular systems with higher concentration these interactions can be taken into account by introducing the structure factor *S(q):*

$$I(q) = nP(q)S(q) \qquad \text{(Eq.7)}$$

With *P(q)* as the form factor denoting the intra-particle contributions and *n* as the particle concentration (number of particles per volume).

The structure factor depicts the average spatial arrangement of the particles. For a non-interacting system (high dilution) *S(q)* would be 1 over the whole q-range. The structure factor is calculated by using different structure factor models which are defined by different sets of parameters. For example the monodisperse hard spheres, charged spheres, attractive spheres and lamellar phases are included in the GIFT software. To find the best parameters for the fit a Boltzmann simplex simulated annealing algorithm is used. Physically reasonable limits have to be set to keep the parameters in a realistic range. Details of the IFT and GIFT are well described in the works of Brunner-Popela, J. et al.[21,22], Bergmann et al.[23], Fritz,G. et al.[24], Innerlohninger,J. et al.[25], and Frühwirt et al.[26].

Pattern recognition

GIFT is used to assist the analysis of the structure of particle systems (averaged size or shape) of solid and liquid samples. The method is e.g. applied to interpret data from small angle x-ray scattering (SAXS) experiments.

In general different liquid crystal phases (EME, H_2, Fd3m, Pn3m) can be differentiated because of the relative positions of their scattering peaks in the scattering functions. The determination of the phase can be done by a program called SGI (Space Group Indexing). This is well described in Guillot et al.[27]

For lamellar systems the pattern recognition is relatively easy due to their equidistant peaks. The structure factor (S(q)) provides information not only about the ordering of the bilayers but also about the bilayer flexibility and the number of coherently scattering bilayers. The form factor (P(q)) is related to the thickness and the internal structure of one single bilayer.[26]

For hexagonal systems the interpretation becomes more complicated. The pattern is no longer equidistant but the peaks appear at the relative positions $\sqrt{1}, \sqrt{3}, \sqrt{4}$ in the scattering curve. When the hexagonal system is treated as accumulation of cylinders with the assumption of no specific orientation, their length being rather large compared to their cross section and a negligible polydispersity it is possible to use GIFT in combination with a deconvolution method (DECON). This is described well in Freiberger et.al.[28]. However, a GIFT evaluation is not possible for the ISAsome systems used in this work due to the weak order in the system. So we could only apply the SGI routine. An example of the determination of a hexagonal system from the scattering curve using the SGI is given in Figure 5.
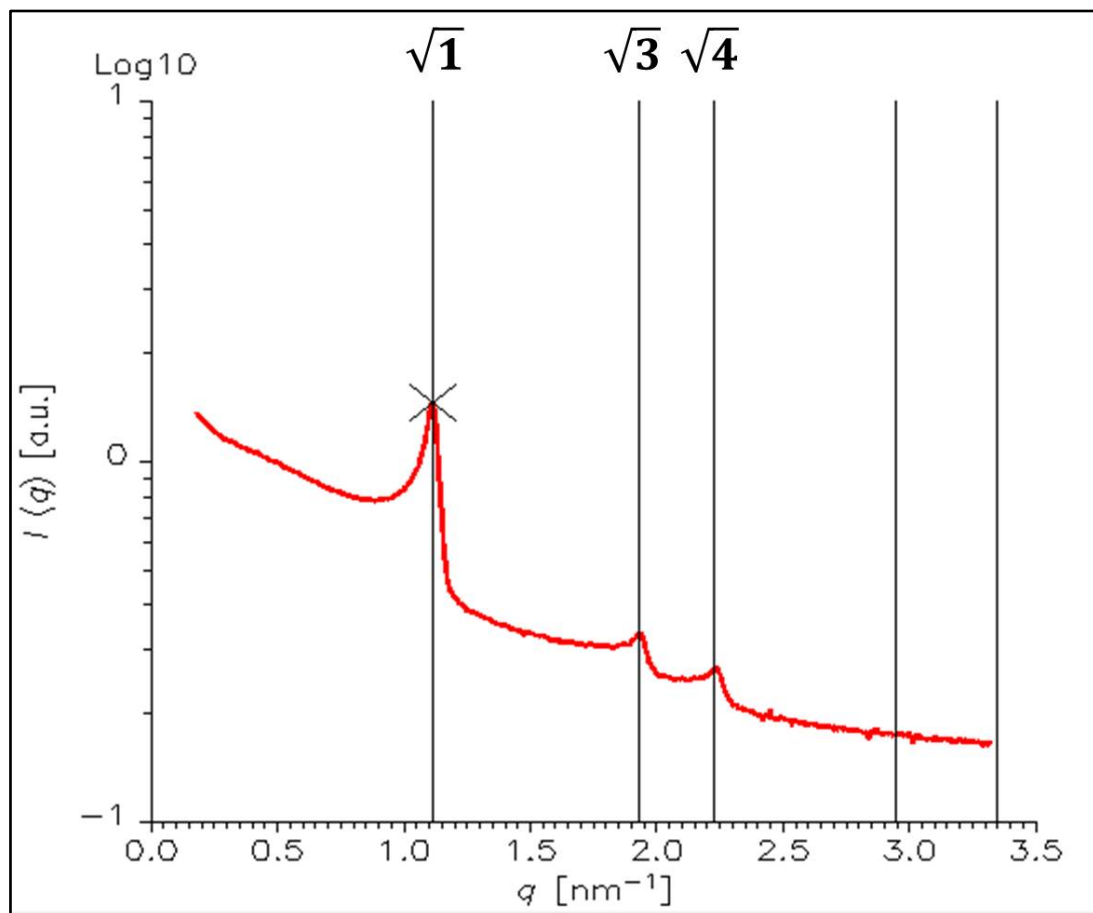

Figure 5: Example of space group indexing of a hexagonal phase.

Light Scattering

In a scattering experiment an incident beam is sent through a sample holder and the light is scattered by the sample. A detector is positioned at a certain angle to the incident beam (scattering angle θ) where it measures the intensity of the scattered radiation I(θ,t).

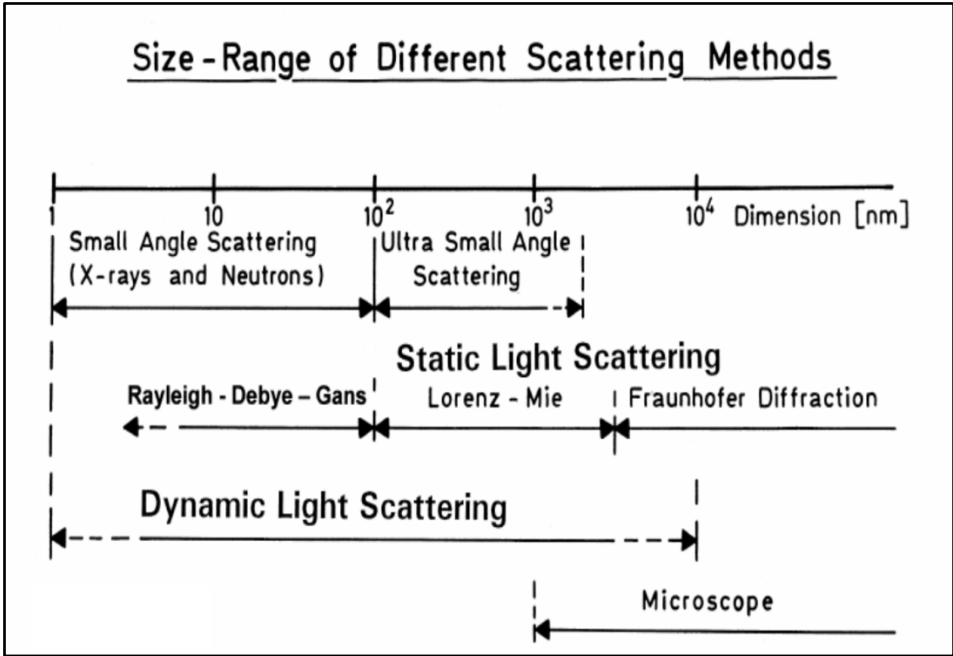Depending on the radiation source (wavelength λ) different size regimes can be measured (Figure 6).

Figure 6: Different size regimes of different scattering methods

Since we want to investigate a novel light scattering method within this work, we look at the theory of Light Scattering particularly Dynamic Light Scattering (DLS).

Every excitable center (electrical dipole in light scattering) emits scattered radiation of certain intensity. For light scattering this intensity is proportional to the square of the refractive index difference (number of polarizable electrons).

First we want to differentiate between Static Light Scattering (SLS) and Dynamic Light Scattering. (Figure 7)
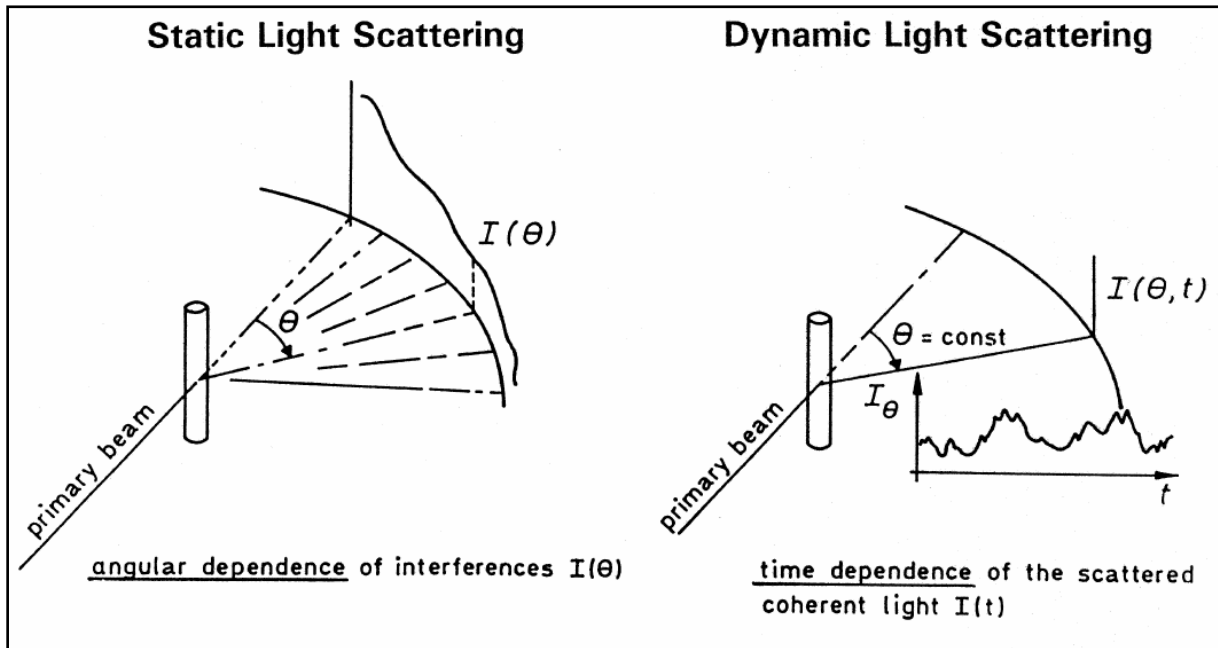

Figure 7: Schematic representation of static (left) and dynamic (right) light scattering

In SLS information about the shape of particles and interactions of different particles can be obtained by investigating the angular dependence of the time averaged scattered intensity. The intensity is measured over an angular range, typically between 10° and 150° limited by the primary beam the optical components and the cell geometry.

SLS is usually used employing the Lorenz-Mie theory[17] where the size of the scatterers is comparable to the wavelength. With this method it is possible to measure particle sizes in the range of 10^2 nm up to several μm. With the Rayleigh-Debye- Gans theory, which is also valid for x-ray and neutron scattering it is possible to measure particles if the following condition is fulfilled

$$2\alpha(m - 1) \ll 1 \qquad\qquad\text{(Eq.8)}$$

where α is the size parameter (2πR/λ) and m the ratio between the refractive indices of the particle and the solvent (n_P/n_S).

Since λ and R (radius of a sphere- particle dimension) is usually preset it is possible to tune the *m* value by partially index matching the refractive indices. The above condition is easily fulfilled for very small particles.

In dynamic light scattering the time dependent fluctuation of the scattering intensity at a fixed angle is measured. If a coherent primary beam (laser light) is used, information about the dynamics of fluid systems can be obtained, as long as they are in the ergodic regime (time average = ensemble average). In most applications DLS is used for the determination of the particle size. This can be done in the range of nanometers up to several micrometers. The samples have to be highly diluted, so multiple scattering is avoided.

The fluctuations of the intensity are caused by the Brownian motion of the particles. Consequently their phases are time dependent. The total scattering field is calculated by summing over all individual scatterers (N_S)

$$E_S(q,t) = e^{i2\pi vt} \sum_{i=1}^{N_S} e^{-iqr_i(t)}$$ (Eq.9)

with v as the frequency of the light. As described above the scattered field is not experimentally measurable, so we need the complex square of this function which is the intensity *I(q,t)*.

To describe the fluctuations of the intensity we use the ACF (autocorrelation function). *$G_2(\tau)$* is the intensity autocorrelation function

$$G_2(\tau) = \langle I(0)I(\tau) \rangle = \lim_{T \to \infty} \frac{1}{T} \int_0^T I(t)I(t+\tau) \, d\tau$$ (Eq.10)

T is the measuring time which has to be larger than the fluctuation time and τ is the correlation time. It should be mentioned here that available correlators usually give the normalized ACF:

$$g_2(\tau) = \frac{G_2(\tau)}{\langle I(t) \rangle_{time}^2} - 1$$ (Eq.11)

This normalization to 1 is mathematically reasonable because the ACF depicts probabilities. A disadvantage of the normalization is that it is not possible to represent the actual scattered intensity when presenting data.

Note: The substraction of 1 leads to the decay of the correlation function $g_2(\tau)$ from 1 to 0 (before 2 to 1).

The connection of this function to the field correlation function ($G_1(\tau)$) is called the Siegert-relation

$$G_1(\tau) = \sqrt{G_2(\tau) - 1} \qquad \text{(Eq.12)}$$

$G_1(\tau)$ is needed for the evaluation.

The Siegert-relation can also be depicted as

$$G_2(\boldsymbol{q}, \tau) = 1 + \beta |G_1(\boldsymbol{q}, \tau)|^2 \qquad \text{(Eq.13)}$$

β is called the intercept which is usually dictated by the ratio of the speckle size to the detector size (coherence factor). It is also dependent on the alignment and the used method.

For the case of a dilute, monodisperse system (all particles with the same size), an infinite small detector and perfectly coherent scattering the field correlation function becomes

$$G_1(\tau) = e^{-Dq^2\tau} \qquad \text{(Eq.14)}$$

with *D* as the translational diffusion coefficient which is indirectly proportional to the size of the particles, also known as the Stokes-Einstein relation

$$D = \frac{k_B T}{6\pi\eta R_H} \qquad \text{(Eq.15)}$$

where k_B is the Boltzmann constant, T is the absolute Temperature, η is the viscosity of the solvent and R_H is the hydrodynamic radius.

For dilute polydisperse systems the exponential function in Eq. 14 has to be replaced by a weighted sum (integral) where the weight $W(\Gamma)$ denotes the contribution of each population Γ.

$$G_1(\tau) = \int W(\Gamma)e^{-\Gamma\tau}dT \qquad \text{(Eq.16)}$$

where Γ is the product Dq^2 (decay rate of the function) and all amplitudes of the signal are denoted by the intensity weighted distribution ($W(\Gamma)$).

Since this is a Laplace transformation an inverse Laplace transformation is necessary to derive the amplitudes of the individual decay rates from the correlation function. Furthermore it is possible to use the relation $\Gamma = Dq^2$ and Eq.15 to calculate the size of the different populations, i.e. to calculate a size distribution.

Basically this is possible in three differently weighted ways, namely Intensity, Mass (Volume) and Number weighted. Where the Mass (Volume) weighted function gives an averaged picture over all present sizes according to their sizes (R^{-3}, assuming a spherical shape), Intensity (or "unweighted" distribution) is very sensitive to larger particle sizes and Number on the smaller particle sizes (R^{-6}). There are several computer programs, like CONTIN, REPES and ORT[29](Optimized Regularization Technique) that were programmed to carry out these transformations. For a classical DLS experiment the sample has to be ergodic and transparent in order to gain the time average and therefore the ensemble average. The correlation function should have low statistical noise to allow for an inverse Laplace transformation. To get good statistics an average of 10^7 counts should be measured.

3D Cross

The 3D cross technique is used as a method to eliminate multiple scattering. In this method the primary beam is guided into a splitter and the two resulting parallel beams (*m,n*) are focused in the sample by using lenses. Two detectors (*i,j*) are mounted to collect the scattered light at the same scattering vector. The corresponding signals are then cross-correlated (see Eq.16).[30]

$$g_2(\tau) + 1 = \frac{\langle (I_i^m(t) + I_i^n(t))(I_j^m(t+\tau) + I_j^n(t+\tau)) \rangle}{4 \langle I_i(t) \rangle \langle I_j(t) \rangle} \qquad \text{(Eq.17)}$$

By correlating $\langle (I_i^m(t) I_j^n(t+\tau) \rangle$, only single scattered light is filtered from the scattered light. In a 3D cross experiment the theoretical limit of the intercept is β = 0.25, because scattered light of both beams can fall into both detectors. This leads to an increase of uncorrelated light. The intercept is of course also influenced by reflections of the instrumental parts, so in a real experiment it is usually around 0.10-0.17. Details of a setup for a 3D cross experiments are described elsewhere.[12]

Ergodic vs. nonergodic systems

It is important for DLS techniques to differentiate between ergodic and nonergodic systems. Ergodicity means that particles (droplets) can move freely in the sample with the highest degree of freedom. By increasing the viscosity of the system, e.g by adding gels which form 3D networks, the system is still ergodic until the transition point is passed, where the particles are, at least partially, fixed in space and time.

In an ergodic system the particles will, with time, experience all possible configurations and so the ensemble average is simply given by the time average:

$$G_{Ensemble}^2(\boldsymbol{q}, \tau) = G_{Time}^2(\boldsymbol{q}, \tau) \qquad \text{(Eq.18)}$$

In a nonergodic system at least a portion of the scatterers cannot diffuse freely anymore and then the time average will not give the ensemble average:

$$G^2_{Ensemble}(\boldsymbol{q}, \tau) \neq G^2_{Time}(\boldsymbol{q}, \tau) \qquad \text{(Eq.19)}$$

This means that the Siegert relation (Eq.12) is no longer valid, meaning that it is not possible to calculate the ensemble averaged field correlation function from the time averaged intensity correlation function. In other words, each speckle leads to a different correlation function. If a sufficient number of speckles (~10^3) are measured, the weighted average over these speckles will result in the ensemble averaged intensity correlation function again. To achieve this special experimental procedures have to be used to measure the ensemble average, i.e. the brute force technique for short correlation times and the echo technique or the multispeckle method for long correlation times.

Brute Force

The Brute Force method poses a possibility to obtain the ensemble average in a nonergodic system. This is achieved by moving the scattering volume in the sample and measuring repeatedly at different positions and therefore speckles. Coupled with the ECHO technique this is done by rotating the flat cell stepwise, not in a continuous rotation. Coupled with the Multispeckle technique the flat cell is moved linearly stepwise in the vertical direction (see Materials and Methods). By averaging over the time averaged correlation functions ($G_2^i(\tau)$) of many such measurements the ensemble average can be obtained. If one channel is used:

$$g_2(\tau) = \frac{M \sum_{i=1}^{M} G_2^i \langle I_i(t) \rangle^2_{time}}{(\sum_{i=1}^{M} \langle I_i(t) \rangle_{time})^2} - 1 \qquad \text{(Eq.20)}$$

M is the number of single measurements (speckles). Figure 8 shows the application of Eq. 20 on $G_2^i(\tau)$ time averaged correlation functions of single measurements and the resulting ensemble averaged intensity correlation function.
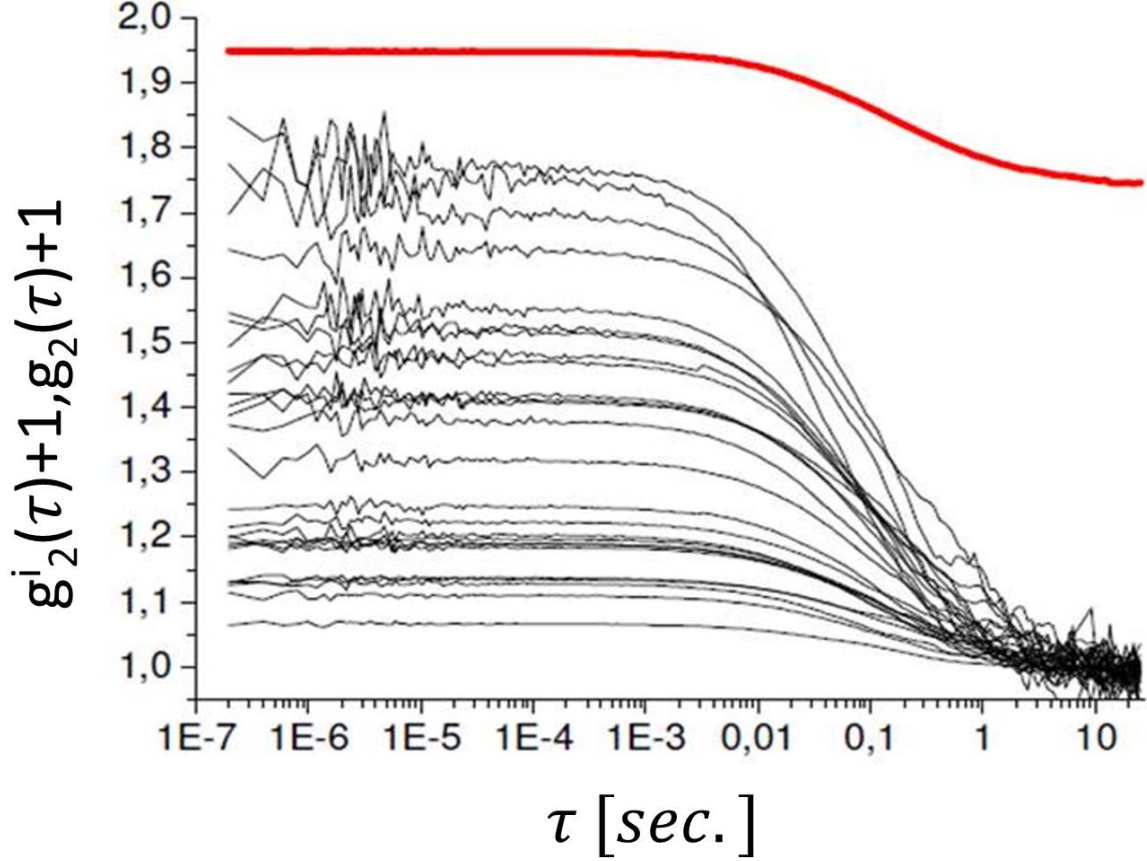
In the case of pseudo cross-correlation (two channels) we have to use the following equation

$$g_2(\tau) = \frac{M \sum_{i=1}^{M} G_2^{ab} \langle I_i(t)\rangle_a \langle I_i(t)\rangle_b}{\sum_{i=1}^{M} \langle I_i(t)\rangle_a \sum_{i=1}^{M} \langle I_i(t)\rangle_b} - 1 \qquad \text{(Eq.21)}$$

Where M is the number of single measurements, G_2^{ab} is the time averaged cross-correlation function of each single measurement. $\langle I_i(t)\rangle$ is the averaged intensity of each single measurement and the indices a,b depict the two different channels. Correlation times in nonergodic systems can be 10^4 s and more.

Since it is usually necessary to carry out several 100 measurements to get good statistics, the complete measurement time can become unreasonably long. For this reason the Brute Force method is mostly used to obtain information about the short time dynamics ($\tau \leq 1s$), typically up to a few seconds. These results have then to be combined with results from the Echo- or Multispeckle method.

ECHO-Method

The echo method [30,31,32] can be used to determine long term dynamics of nonergodic systems up to 10^4 s In order to achieve this, the sample is rotated constantly so that speckle 1 (yellow point in Figure 9) is at the same position after one revolution (360°). The revolution time (τ_R) depends on the speed of the motor, which also determines the minimum τ_R ($\geq$ 1 sec). The other speckles follow with the according time difference. The signal is averaged over all speckles on the circle leading to the ensemble average. While the sample is rotating the intensity is measured every τ_S sec (usually 20 – 1200 µs). To obtain the correlation function for τ_R the measured intensities in τ_S around the τ_R are correlated.
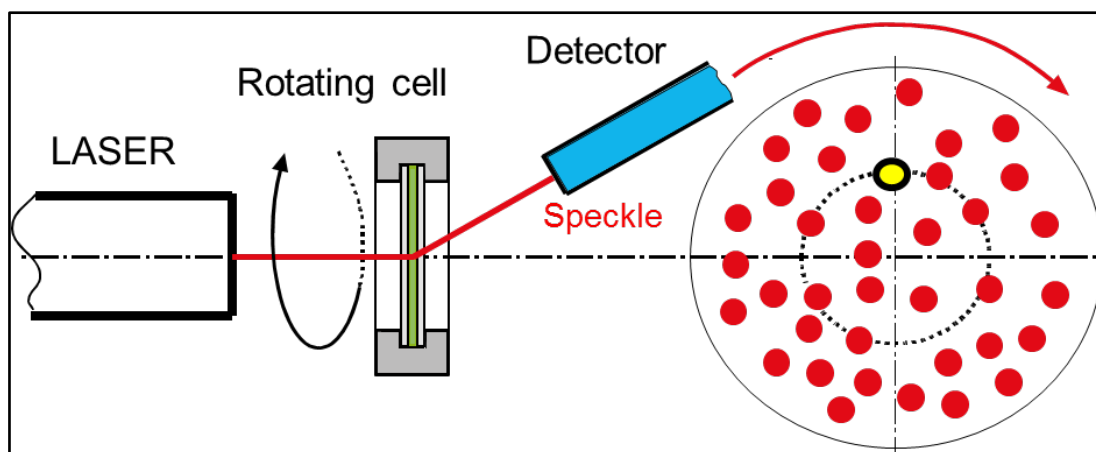

Figure 9: Schematic depiction of the echo method[30]

Since the detection area should always be smaller than the speckle size, there is a certain time period in which one speckle enters the detection area and leaves it. The

signal that derives from one speckle is highly correlated. However the neighboring speckles are completely uncorrelated. The echo peaks (see Figure 10) are derived by averaging over all speckles and revolutions of the sample. The decay of the peak maxima over time is the correlation function.[30]
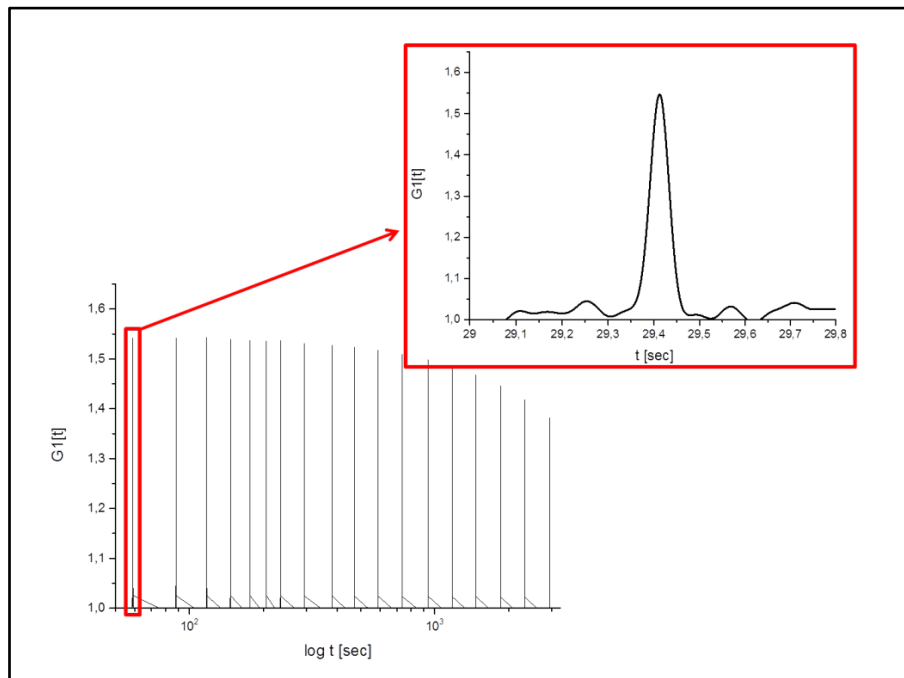

Figure 10: echo peaks, and zoom on the first detected peak.

As it will be described in more detail in Materials & Methods the rotation of the cell has to be very precise. To accomplish a perfect rotation is practically impossible. There will always be slight deviations, but they can be corrected. To do this we look at the Zero Echo (see Figure 11).

If rotational imperfections are present the area of all echoes are not affected. However their maxima will decrease and their width will increase. This is not the case for the Zero Echo (see Figure 11). In other words the pure dynamics of a sample can be determined via the relation of the area under the nth echo and the area under the Zero Echo.

With this knowledge the correlation function can be obtained by

$$G_{corr}(\tau_n) = \frac{A_n}{A_0}(G(0) - 1) + 1$$

(Eq.22)

with $\tau_n = n * \tau_R$, A_0 and A_n the areas under the zero echo and the nth echo and G(0) the maximum of the zero echo. G(0) can also be used to estimate the intercept.
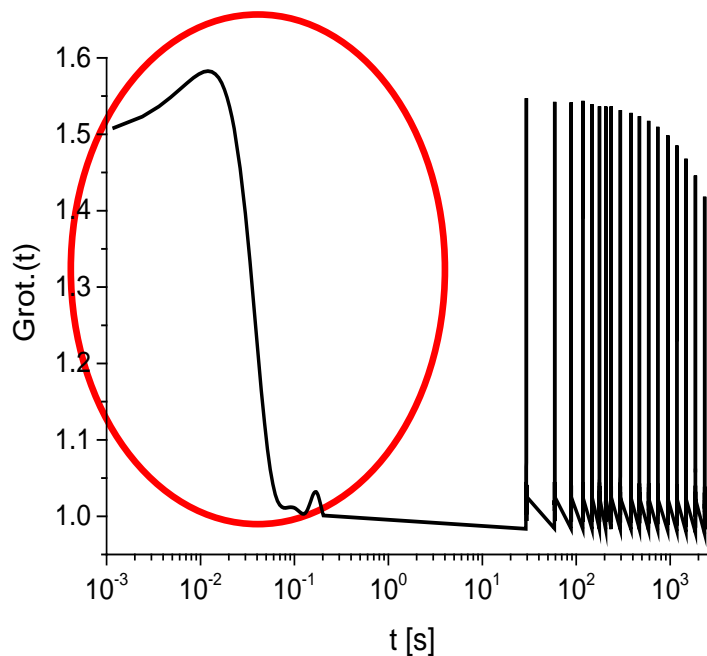

Figure 11: Zero Echo

To calculate the area under the echo there are three established methods. The best of the three is to choose a fixed interval around the peak maximum. A description of all three methods can be found in [31].

With equation 22 relative small deviations can be corrected. To test the quality of the rotation and therefore prove that equation 22 is applicable the FWHM (full width at half maximum) function relative to the zero echo can be used.

Basically the relative FWHM has to be smaller than 2. If it gets bigger than 2, all following echoes cannot be used. In addition, if a double peak appears or the peak is asymmetric, the data should not be used.

Multi-tau scheme

In a standard DLS experiment the stochastic signal is correlated over logarithmically increased lag times (τ). The time the correlator needs to count and readout the Intensity (photon count) is the sampling time (Δt). The time between Δt and τ is the delay time (k). If Δt is constant k increases with increasing τ, and the dynamical information in this increasing time frame is lost.
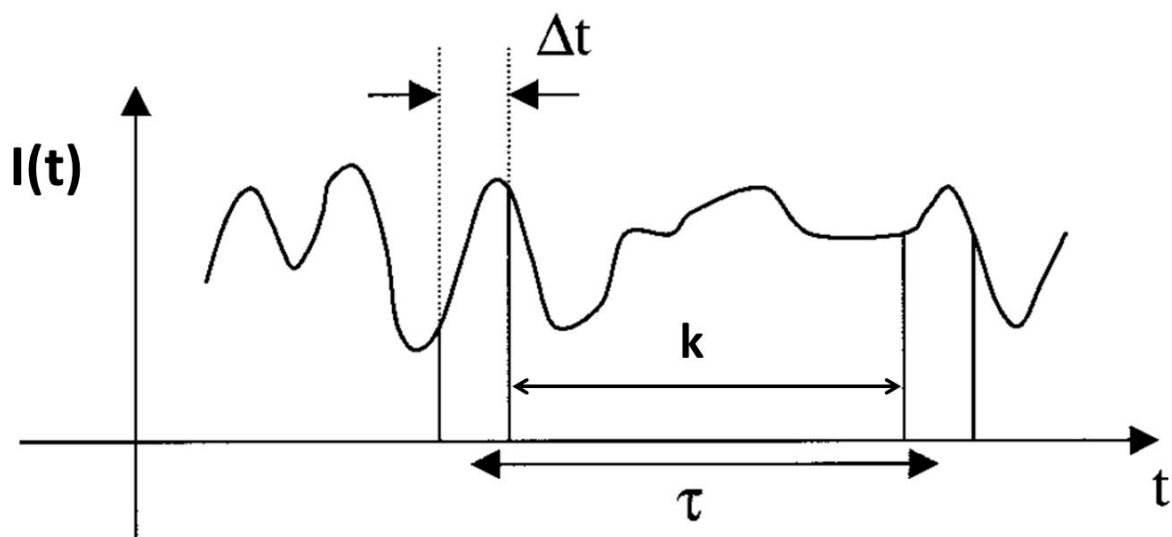
Figure 12: Scheme of the photon count (I(t)) plotted against time (t) in a DLS experiment. τ – lag time; Δt – sample time; k – delay time.[33]

Schätzel et al.[34] found a way to use this "lost" information, by increasing Δt proportionally for increasing τ, introducing the multi tau scheme.

Since this method is used for ergodic systems (speckles move), the averaging of neighbouring speckles is the result. It is not applicable to an echo measurement, where it is necessary to correlate the intensity of one speckle with the intensity of the same speckle over and over again for a long time.

K.N. Pham found a way to apply the multi-tau scheme to echo DLS. He achieved an increase of the sample time by averaging the intensities of the same speckle at consecutive revolutions, giving a new "sample". This new sample stream is then correlated with an effectively doubled sample time (Δt). [32]

CCD / Multispeckle

The Multispeckle method is used to measure the long time dynamics in a range of 1 sec (depending on the quality of the camera also below 1 s) up to 10^5 s. The main difference between a standard dynamic light scattering experiment and a multispeckle experiment is the detector. As the name already suggests the detector area is huge compared to the standard, and many independent speckles ($>10^3$) are monitored at the same time. Usually a CCD camera (charged coupled device) is used. A main parameter for the quality of this technique is the speckle/pixel ratio. This has always to be larger than 1, because if one pixel sees several speckles, the intensity fluctuation will average out.

If the speckle size is much bigger than the pixel size (n-times), the signal of n x n neighbouring pixels can be averaged to one "averaged pixel". The speckle size is inverse proportional to the scattering volume and can be adjusted by the laser beam diameter.

By correlating the pictures that are taken by the CCD camera at the chosen time interval (τ), the intensities of many speckles are correlated. This can be seen as the execution of many independent DLS experiments at the same time. Therefore it is possible to extract the ensemble average.

$$g_2(\tau) = \langle \frac{\langle I_{pixel}(t) I_{pixel}(t+\tau) \rangle_{pixel}}{\langle I_{pixel}(t) \rangle_{pixel} \langle I_{pixel}(t+\tau) \rangle_{pixel}} - 1 \rangle_{time} \qquad \text{(Eq.23)}$$

$<...>_{pixel}$ denotes the average over all averaged pixels of one picture. A schematic presentation of the Multispeckle method is shown in Figure 13.
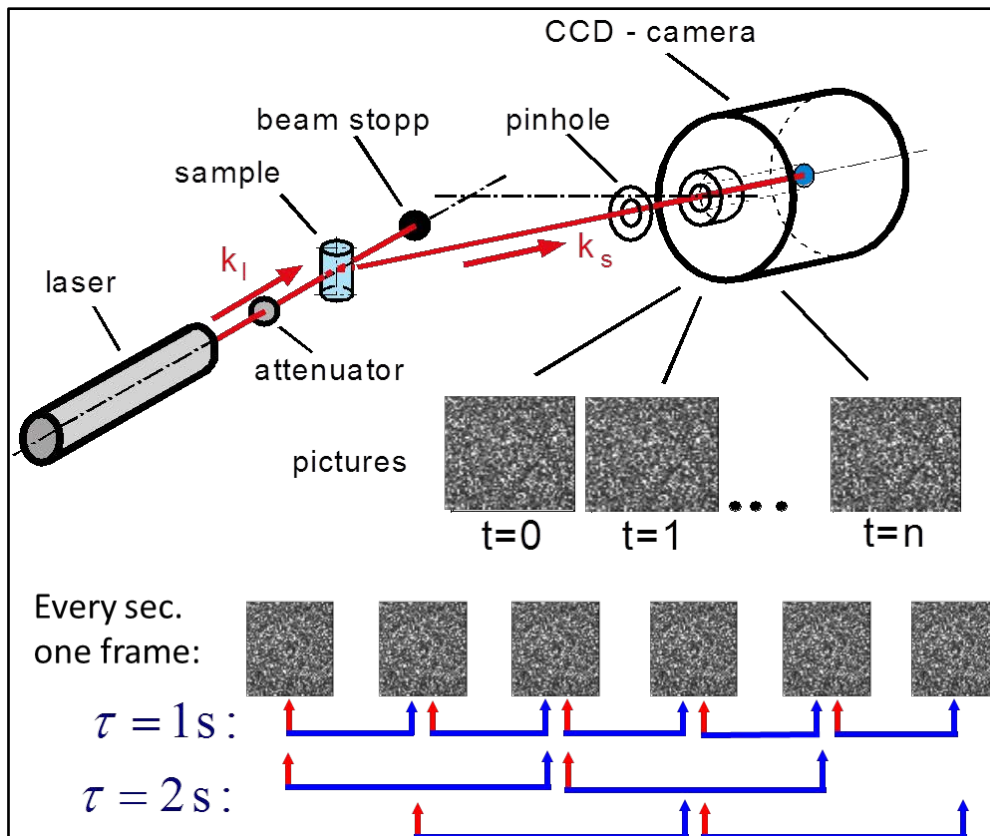
Figure 13: schematic depiction of a Multispeckle experiment[30]

The limiting factor of this method is, as mentioned above, the repetition time between taking the photos (τ_R). To obtain the correlation function below τ_R an alternative method, like Brute Force, has to be used. It should be mentioned here that there is another possibility to obtain the correlation function for time differences below τ_R.

This method is called Speckle Visibility Spectroscopy and is explained in the work of R. Bandyopadhyay et al.[35] As the name indicates the contrast of the speckle pattern is of special interest in this method. This is the case when the motion of the scattering site is much slower than the exposure time of the camera. The essence of this method is not to correlate between images, but to connect the dynamics in a sample to the variance of intensity of the pixels for a particular exposure time, i.e. for exposure times much shorter than the decay time (or lag time, τ) the speckle contrast will be very good, and for longer exposure times (speckles change) the contrast will decrease due to the averaging.

Materials & Methods

ISAsomes Definition

To test the novel techniques we used internally self-assembled liquid crystalline lipid particles (ISAsomes), which are well described in different works by de Campo et al.[36] and Yaghmur et al[5]. In general the term describes a hierarchically ordered colloidal system. The sub-micrometer sized droplets are kinetically stabilized in a continuous water phase with self-assembled internal structures.

The lipid phase was produced by mixing a monoglyceride with ordinary oil, in this case tetradecane ($C_{14}H_{30}$). The used monoglyceride was Dimodan® U/J, Material no. 015312 (DU), donated by DANISCO A/S (Braband, Denmark) comprised of 96% monoglycerides with 62% linoleate and 25% oleate. Tetradecane (TC) was purchased from Sigma-Aldrich with a purity of ≥99.0%, olefin free. For the stabilization of the system the triblock copolymer Pluronic® F127 (PEO_{99}-PPO_{67}-PEO_{99}) was used, which was donated by BASF (U.S.A.).

To arrest the system to a nonergodic state, technical grade κ-carrageenan (KC) was used as a gelling agent.

To define the lipid phase we want to produce, we introduce the δ - value (Eq.24).

$$\delta = \left[\frac{mass\ of\ DU}{mass\ of\ DU + mass\ of\ oil\ (TC)} \right] 100 \qquad \text{(Eq.24)}$$

Depending on the temperature and the δ - value we can choose the phase (see Figure 14).
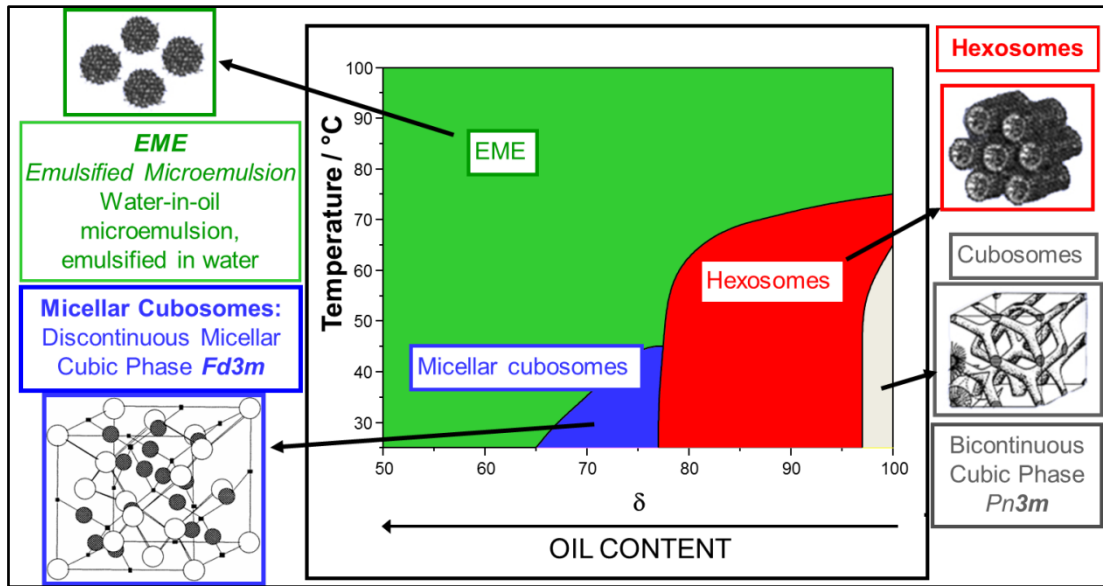
Figure 14: Internal structure of ISAsome emulsions, depending on the temperature and the δ - value.[27]

Furthermore we define the β - value to adjust the amount of stabilizer used.

$$\beta = \left[\frac{mass\ stabilizing\ agent}{mass\ of\ lipid\ phase}\right]100 \qquad \text{(Eq.25)}$$

We used a standard *β* - value of 9.

ISAsomes Preparation

An example of how to prepare a 10 % Isasome emulsion is given in Table 1.

Table 1: Preparation of a 10% Isasome emulsion with β=9

Phase	δ- value	DU (Dimodan U)	+	TC (Tetradecane)	=		in	F127 (1%)
		g		g		g		g
H_2	84	0.84	+	0.16	=	1.0	in	9.0
Fd3m	70.5	0.705	+	0.295	=	1.0	in	9.0
EME	57	0.57	+	0.43	=	1.0	in	9.0

The DU was heated (~ 60°C) to allow homogeneous mixing with TC.

Beforehand the stabilizer was added to the water phase in the proper amount and dissolved under stirring at room temperature (~1.5 h).

The two phases were mixed accordingly (Table 1).

A total of 10 mL sample was prepared in a 20 mL vial. The final mixture then was ultrasonicated for 5 min in pulsed mode (1.5 s on, 0.5 s off) with amplitude of 30% (Vibra-Cell, Sonics & Material, Newtown, CT, USA). During the sonication the samples were positioned in a water bath, because it was found that especially the EME is influenced by the higher temperature that occurs due to the sonication.

The gelling agent was prepared independently, by dissolving the desired amount of KC in water under heating (~65°C) and stirring.

The final concentration of Isasome / KC was achieved by preparing the double of the desired concentration and then mixing the two solutions in a ratio 1 : 1. Final gel concentrations of 0.50 %, 0.60 %, 0.65 %, 0.70 %, 0.75 %, 1.0 % and 2.0 % were produced.

Final ISAsome concentrations of 0.5 %, 1.0 %, 1.5 %, 2.0 %, 2.5 %, 10 %, 20 % and 30 % were produced.

For homogeneous blending of the gel phase and the ISAsome phase and the filling of the flat cell the phases were heated (~60°C).

Light Transmission

To measure the light transmission of different ISAsome concentrations the lab built Flat Cell Light Scattering Instrument (FCLSI) was used. DMSO (Dimethylsulfoxide) was used as index matching fluid. After passing the sample the primary beam is attenuated and its intensity measured with a photodiode and compared to the transmittance of distilled water. Details of the setup can be found in Lehner, D. et al.[37].

Dynamic Light Scattering

For the analysis of the droplet size with DLS a green diode pumped laser (Verdi 5W, Coherent) with a wavelength of 532 nm was used. The typical laser power used was between 0.15 - 0.25 W for each sample. Decalin (Decahydronaphthalin) was used as index matching fluid.

The detector consisted of a single mode fiber (OZ from GMP, Zurich, Switzerland), a photomultiplier detector combined with pseudo-cross-correlation and an ALV5000/E correlator with fast expansion (ALV, Langen, Germany).

To measure the droplet size the samples were highly diluted (4000 times directly before measurement) and the correlation functions were recorded 10 times for 30 seconds each. After averaging them to get the final correlation function a second order cumulant fit[38] was used to determine the mean diffusion coefficient and to calculate the mean hydrodynamic radius (R_H).

Flat Cell

The flat cell was used to decrease the light path through the sample and therefore reduce multiple scattering considerably (see Figure 15). To allow for a smooth measurement, it is crucial that the two glass plates are completely parallel. The sample volume can be tuned by using distance rings with different thickness.

It is possible to tune the sample thickness from 13 µm up to 500 µm. We used a sample thickness of 100 µm for our experiments.
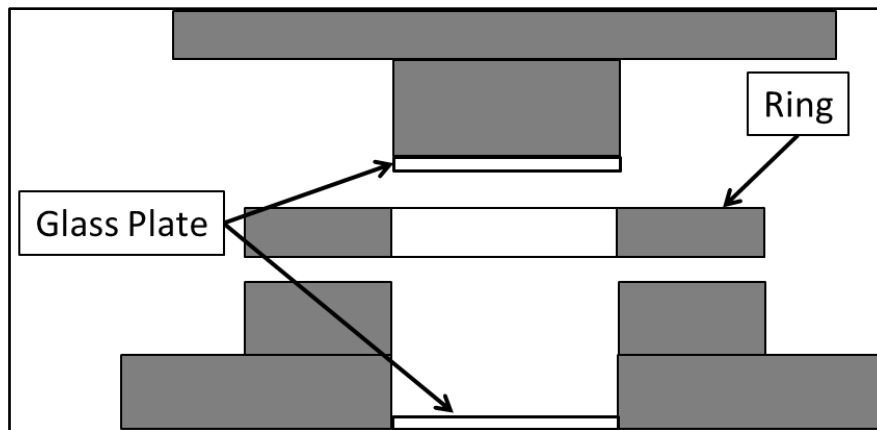
Multispeckle Device

System

The multispeckle device consists of a HeNe laser with 10mW and λ= 632.8 nm (NEC Corp., GFO Germany) and a thermostat controlled sample holder using a flat cell to minimize multiple scattering. The lab built goniometer is equipped with a single mode fiber (OZ from GMP, Zurich, Switzerland), ALV/SO-SIPD/DUAL photomultiplier with pseudo-cross correlation option, and an ALV 5000/E correlator with fast expansion (ALV, Germany) to obtain information about the short time dynamics. On the same goniometer is also a CCD camera, with a 15° offset to investigate the long-time dynamics. The camera- detector distance is 180 mm and the camera itself has a resolution of 640 x 480 pixels with a pixel size of 5.6 x 5.6 µm.

Furthermore the flat cell can be mounted on a linear actuator (Haydon Kerk Motion Solutions, Waterbury, USA) to carry out the brute force technique to measure the short time dynamics in nonergodic systems. The stepper motor is operated by 12 V DC input voltage. The cell can be moved vertically in steps. The step width can be defined by the user. The motor is controlled by the included software IDEA^{TM} and can be connected to the ALV software. The real time setup of the Multispeckle device is shown in Figure 16.

The whole system is placed in a laboratory built "black box" to ensure that no external light can interfere with the measurement.
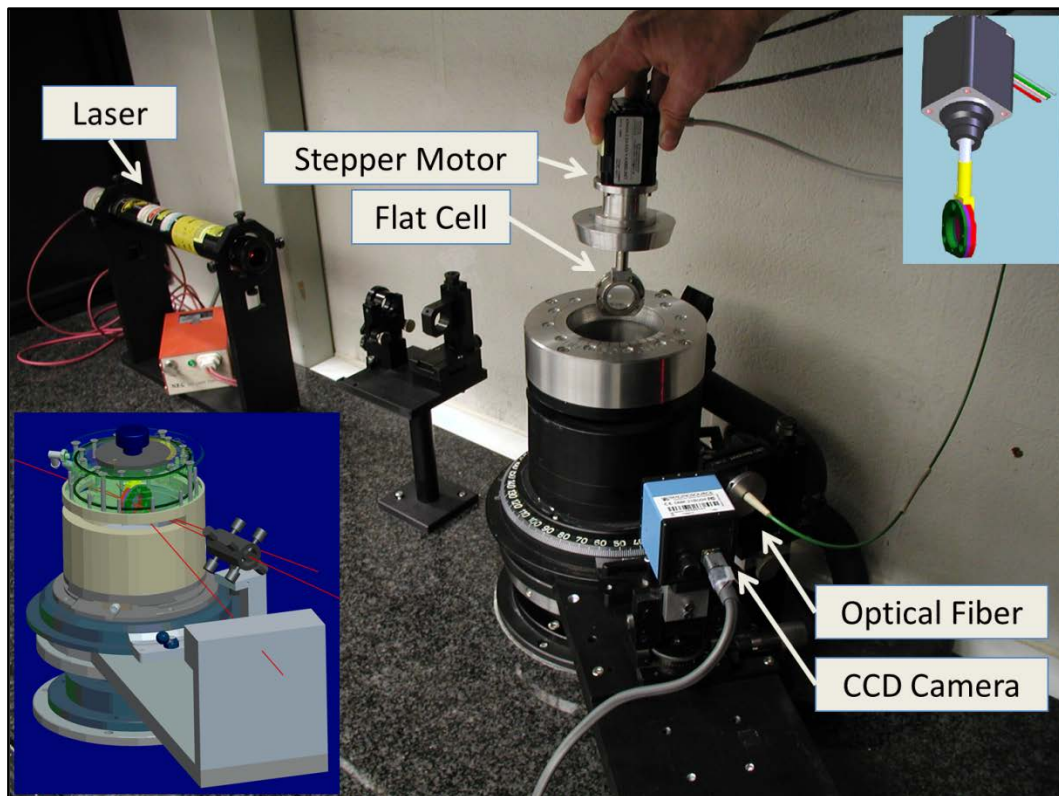
Figure 16: Photo of the Multispeckle device, including schematics showing the setup combined with the CCD camera (gray wall) and an optical fibre holder (left lower corner) as well as the flat cell mounted onto the actuator for the Brute Force measurements (upper right corner).

Motor

The motor is controlled by the program Hydon^{TM} (see Figure 17). The operator can choose the way the motor moves in the vertical direction. Usually the step mode is applied although it is also possible to move the sample in millimeters or inches. Since the motor is connected to the ALV correlation program it is possible to program a sequence the motor executes while the measurements take place in between the steps. So a long term brute force measurement does not need the constant attention of the operator.
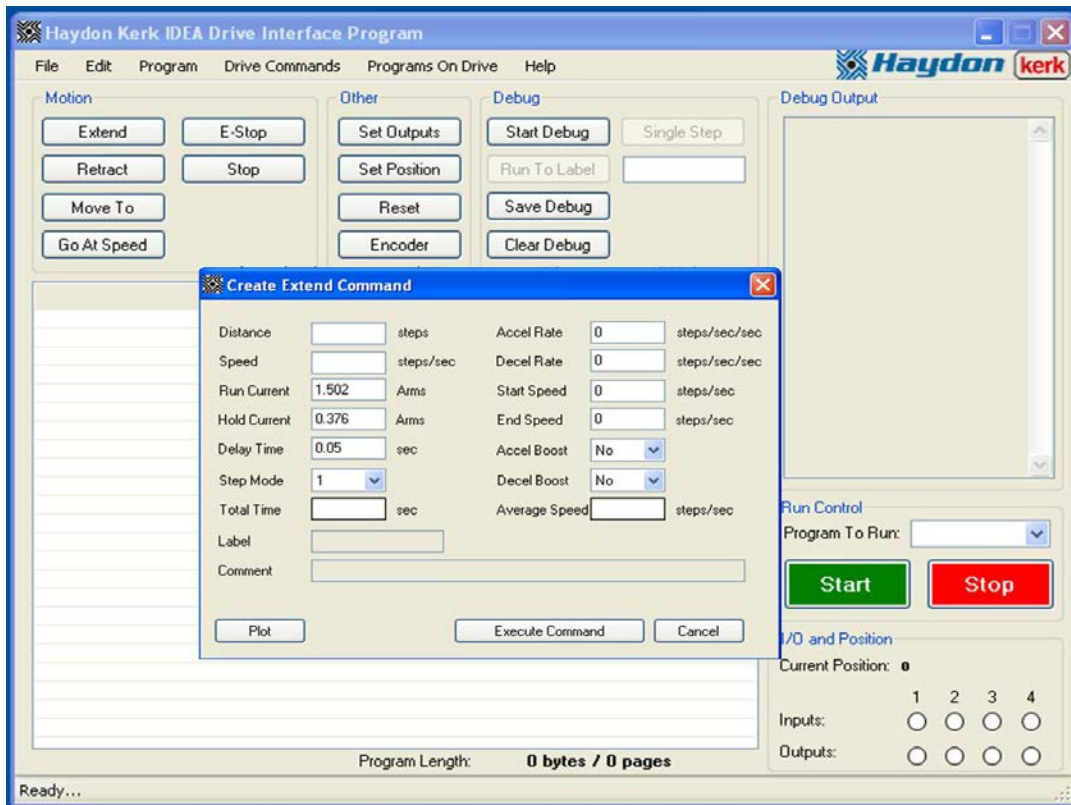
Data acquisition and processing

A multispeckle experiment is controlled and executed by the program IC capture[TM]. For this experiment it is not necessary to move the sample, since many different speckles are recorded simultaneously by the CCD camera.

With IC capture it is possible to change several settings to improve the quality of the measurement:

- Brightness: by increasing the value a constant is added to every pixel value.
- Gain: every pixel is multiplied by a factor
- Exposure: the recording time of each picture
- Gamma control: similar shades of gray cannot be differentiated. The gamma control eliminates this effect.

Furthermore a histogram can be displayed to check the quality of the picture (contrast, intensity, noise) (see Figure 18).
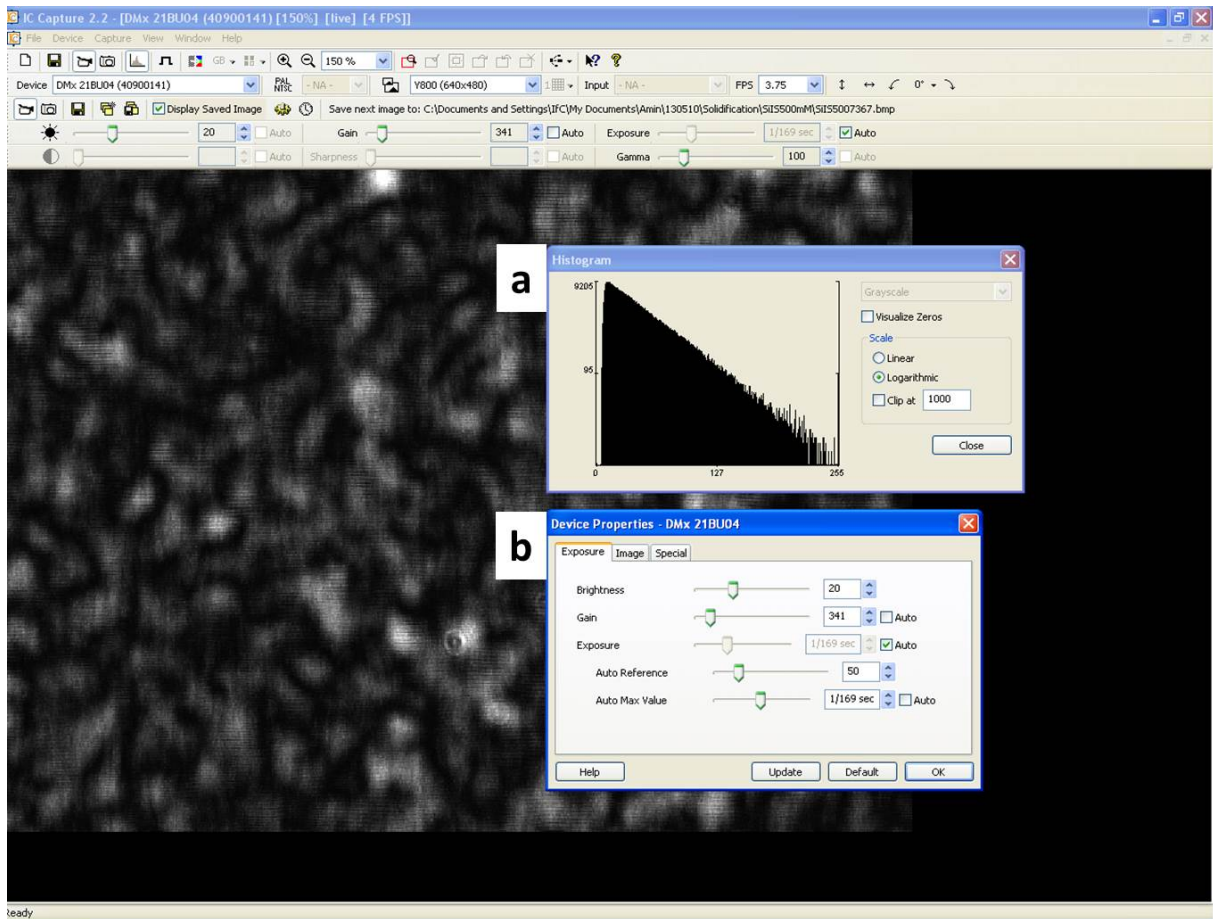
Figure 18: Interface of the IC capture software to execute a multispeckle measurement. a) histogram b) settings[39]
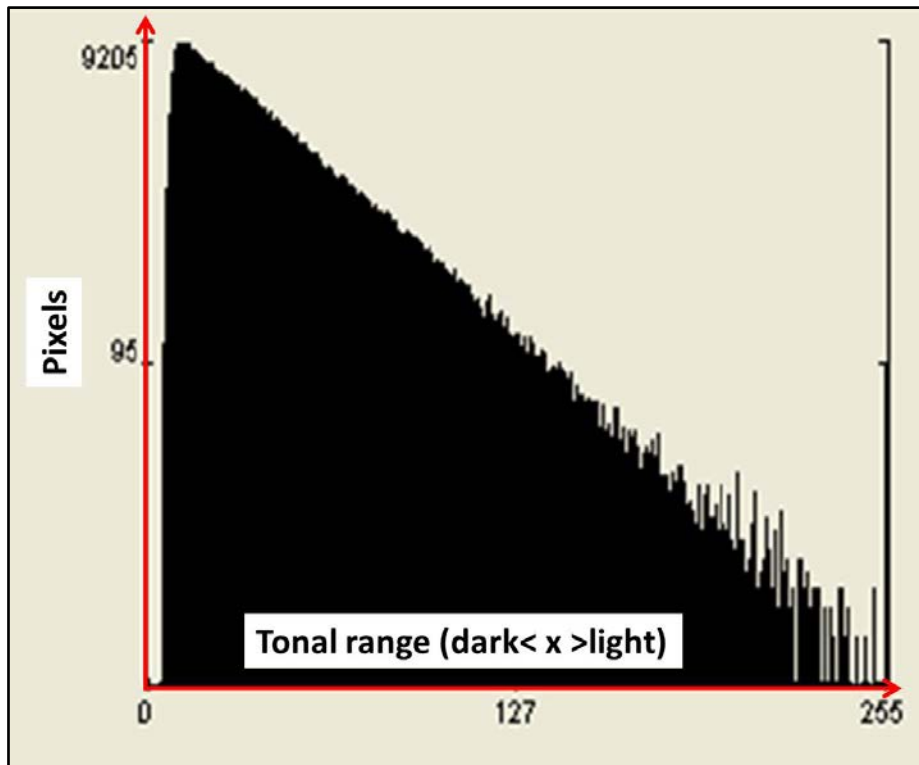

Figure 19: Histogramm

The higher the bar of a tonal value, the more pixels show the corresponding brightness. In Figure 20 two extreme cases with very different brightness settings are shown. None of them are preferable because if too less light enters the camera there is not enough signal, and the available data range of 8 bits is not used. If too much light enters, the contrast is lost because most data points will have an intensity beyond the resolution limit of 255.
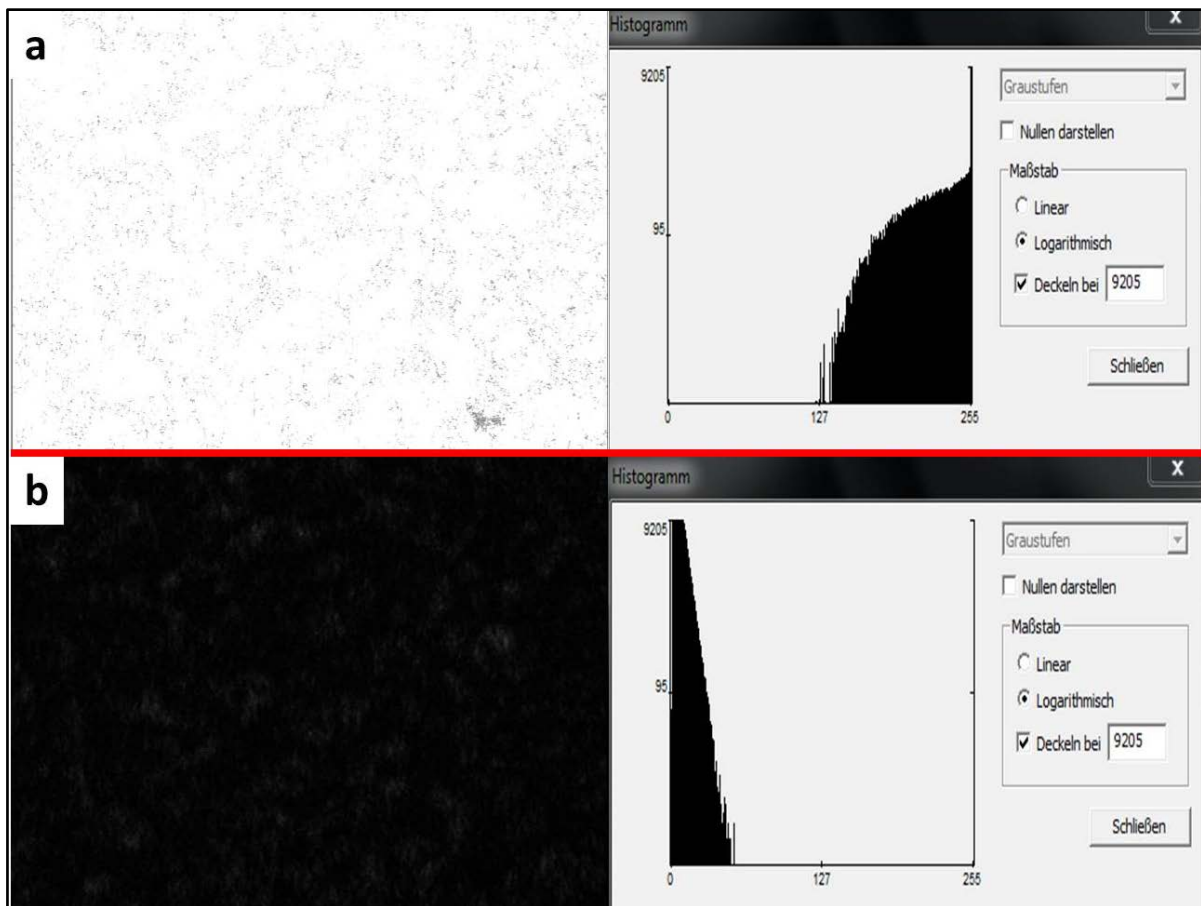
Figure 20: extreme cases of a histogram; a: to high intensity; b: to low intensity

For a multispeckle experiment the histogram should show a linear shape like in Figure 19. Basically a darker picture is advantageous because as mentioned above the contrast is higher.

Correlation and Correction

The collected data are then treated with a correlation program (MSCorr.m), that was programmed by Dr. Amin Sadeghpour and is described in the manual[39].

Due to instrumental reasons the camera shifts a picture now and then, which leads to an overlap. The "damaged" picture has a line in the middle and does not portray one image taken at one time but half the actual image and half the previous or following one.

This is corrected by comparing the pictures to the previous and following ones and deleting them in case of a damaged one.

3D Echo DLS

System

The lab built 3D Echo DLS device consists of a 25 mW HeNe laser (SpectraPhysics) and special 3D optics from LS-Instruments (Fribourg) to use the 3D cross correlation technique to eliminate multiple scattering. By installing crossed polarizers the theoretical intercept (see Chapter Theory, 3D cross) could be improved to $\beta = 1$. In reality intercepts of about 0.6 could be achieved.[40] To detect the signal, single mode fibers from OZ from GMP (Zürich, Switzerland) and an ALV/SO-SIPD/DUAL photomultiplier from ALV-Laser GmbH (Langen, Germany) were used. The device is equipped with a flat cell mounted on a rotating motor to use the echo technique to acquire the long time dynamics. The flat cell was built to reduce the light path through the sample and therefore decrease the amount of multiple scattering considerably. The flat sample cell is installed horizontally to minimize gravitational effects on liquid to viscous samples. The motor, a brushless dc-servo-motor 2444 048B from Faulhaber (Schöniach, Germany) which drives the planetary gear series 14/1 (Faulhaber), can also be used to measure in step mode (Brute Force), to obtain the ensemble average. The motor is regulated by a controller MCBL2805 also from Faulhaber).
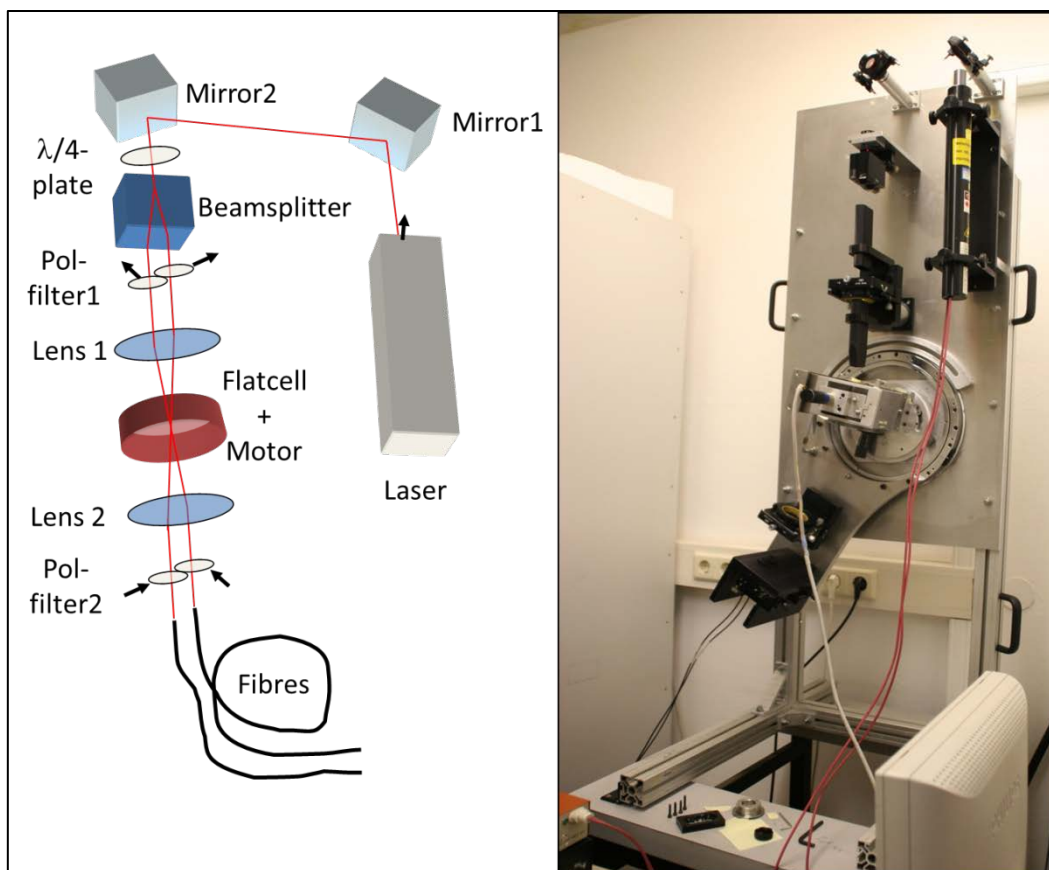
Figure 21: 3D Echo DLS with a flat cell; scheme and photo[41]

The alignment of this lab built device is challenging, and therefore not described in this work. A detailed description can be found in the manual that is available in the laboratory[42].

The goniometer arm is set to the desired angle (up to 35°) and the sample holder to the half of that angle whether you want to measure the brute force method or the echo technique. A simple switch box allows the user to choose between these two methods.

Filling of the flat cell

We heated the sample again to 60 °C, to allow for homogeneous filling of the cell. Most important is to make sure that no air bubbles are trapped in the flat cell. Afterwards the sample was left in the fridge (5°C) for approximately 10 min. following

20 min. equilibration time at room temperature prior to the measurement. Make sure the motor is already running for 30 to 45 minutes to assure a smooth revolution.

Motor

The motor can be controlled with the "motion manager" program to set the desired speed, or to use the brute force technique. Normally two typical rotation speeds are set:

- 1400 rpm (rounds per minute), which corresponds to around 15 s per rotation for correlation times up to 10 000 s and
- 700 rpm (ca. 30s / rotation) for longer times.

Higher rotation speeds are not possible because of the limitation of the bearings and the worm drive. Lower rotation speeds are also difficult because the controller has to work harder to keep the speed constant, which leads to vibrations and therefore the loss of the echo.

A detailed description of the program can also be found in the manual [42].

The motor should be running for about an hour prior to the measurement, to ensure a smooth and shake free revolution.

Data acquisition and processing

For the collection and the correlation of the data different programs are used (Figure 22). These programs are operated via DOS (Direct Operating System) or a batch file.
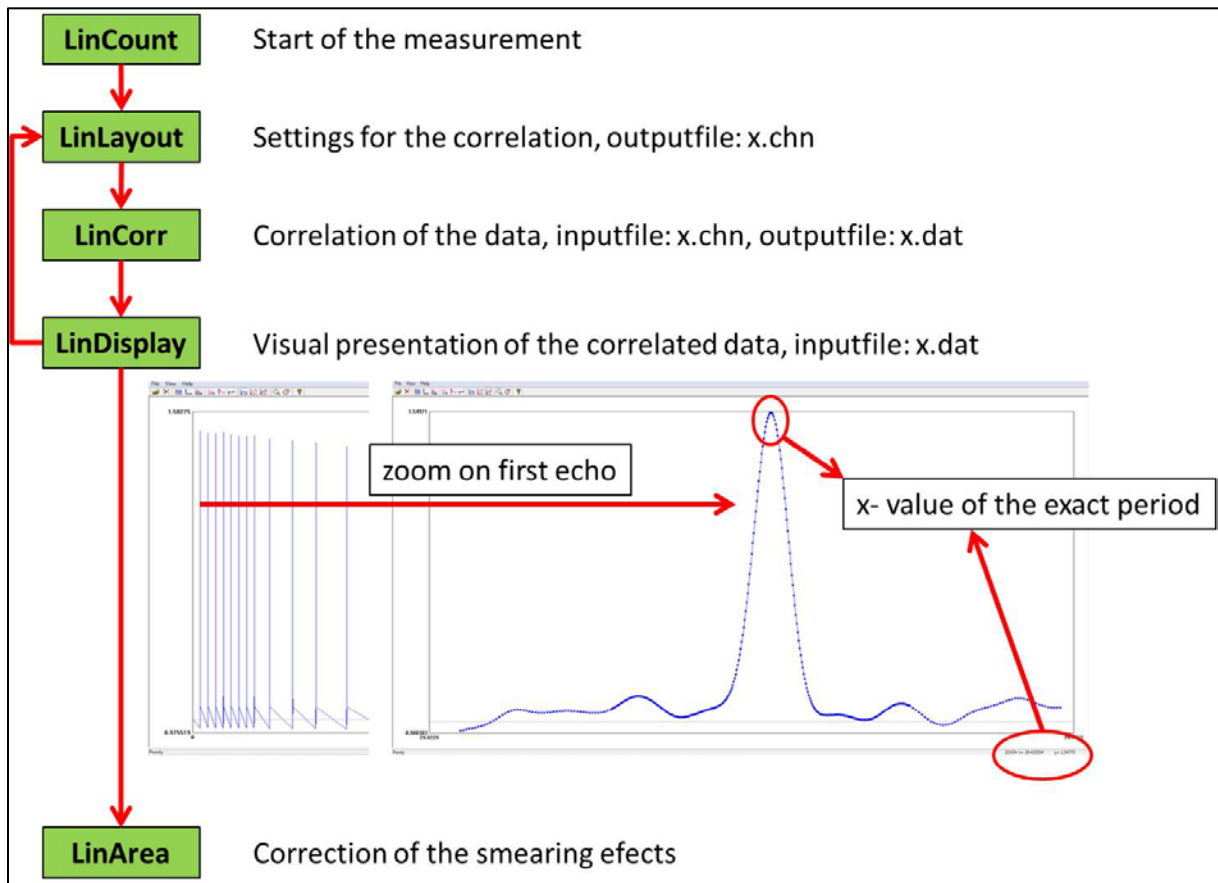

Figure 22: Scheme of the sequence of the programs to execute the echo technique

LinCount: The collection of data is performed by the program LinCount, which converts the photon count and saves it as binary data sequences. The operator has to tell the program:

- Sample time [µs]: defines the interval between two data points
- Duration [s]: total time of the measurement e.g. 15000 (ca. 4 hours)
- File name

LinLayout: With LinLayout the operator creates a file that allows to define the settings for the correlation of the data, like

- Period ([s], the time between two echoes - one full revolution),

- Sample Time ([μs], same as in LinCount),
- number of channels per echo (core and wings- this determines the temporal resolution of the echo),
- first echo number, output format, etc

A detailed description of the different settings and how to define them can be found in the manual[42]

LinCorr: This program is started once the settings are defined. It runs simultaneously with LinCount and allows the operator to correlate the data online, while the measurement is still running. This way it is possible to see if the motor is running without any problems or if the measurement has to be stopped.

LinDisplay: With this program the acquired and correlated data (outputfile from LinCorr) can be displayed. The first entry in LinLayout is only an estimated Period time for the measurement. To get the echo for longer correlation time the exact period time has to be found with the help of this program. By zooming in on the first echo and and identifying its maximum (x-value) the exact period can be found. After entering the new found value into LinLayout and rerunning LinCorr the correlation function should reach higher times than before. It is necessary to repeat this step 2 to 3 times in order to get the whole correlation function.

LinArea: This program is used to correct the smearing effects that occur due to slightly imperfections in the rotation. The correction is done by the normalization of the area (hence the name) under the echoes (see Eq.22, Theory/ ECHO-Method)

Combination of Brute Force and Multispeckle/Echo Data

After we have collected sufficient data of the short term dynamics (Brute Force method) and the long term dynamics (Echo/ Multispeckle technique), it is reasonable to connect this data to show the whole correlation time range from 10^{-7} - 10^{4} s (Echo method) / 10^{5} (Multispeckle method).

From currently available ALV correlation systems the resulting correlation function will be automatically normalized and baseline corrected (e.g.: subtraction of the value 1, see Light Scattering – page 20).

In other words it will decay from 1 to 0 in an ideal case. Due to technical reasons (instrumental imperfections, noise) unity is usually not reached.

After using Eq.20 (or Eq.21 for our pseudo-cross setup) for the Brute Force experiment, the intercept is close to unity (effect of β, see Eq.13). We correct $g_2(\tau)$ by division through β (Figure 23,a). The intercept of the correlation functions of the Multispeckle and Echo technique cannot be relied on because the lower limit of the correlation is $\geq$ 1 second.

In theory long term measurements can be done using the Brute Force method but it is not recommended due to excessively long measurement times. To overlap the Brute Force correlation function with the Multispeckle/Echo correlation function we can however use the time overlap. Since the last data points should be ignored because of the termination effect, for a Brute Force measurement of 600 seconds the reliable overlap regime would be at about 60 seconds. To join the correlation functions from the two methods the Multispeckle/Echo curves are normalized by a corresponding factor. The final result is depicted in Figure 23, c.
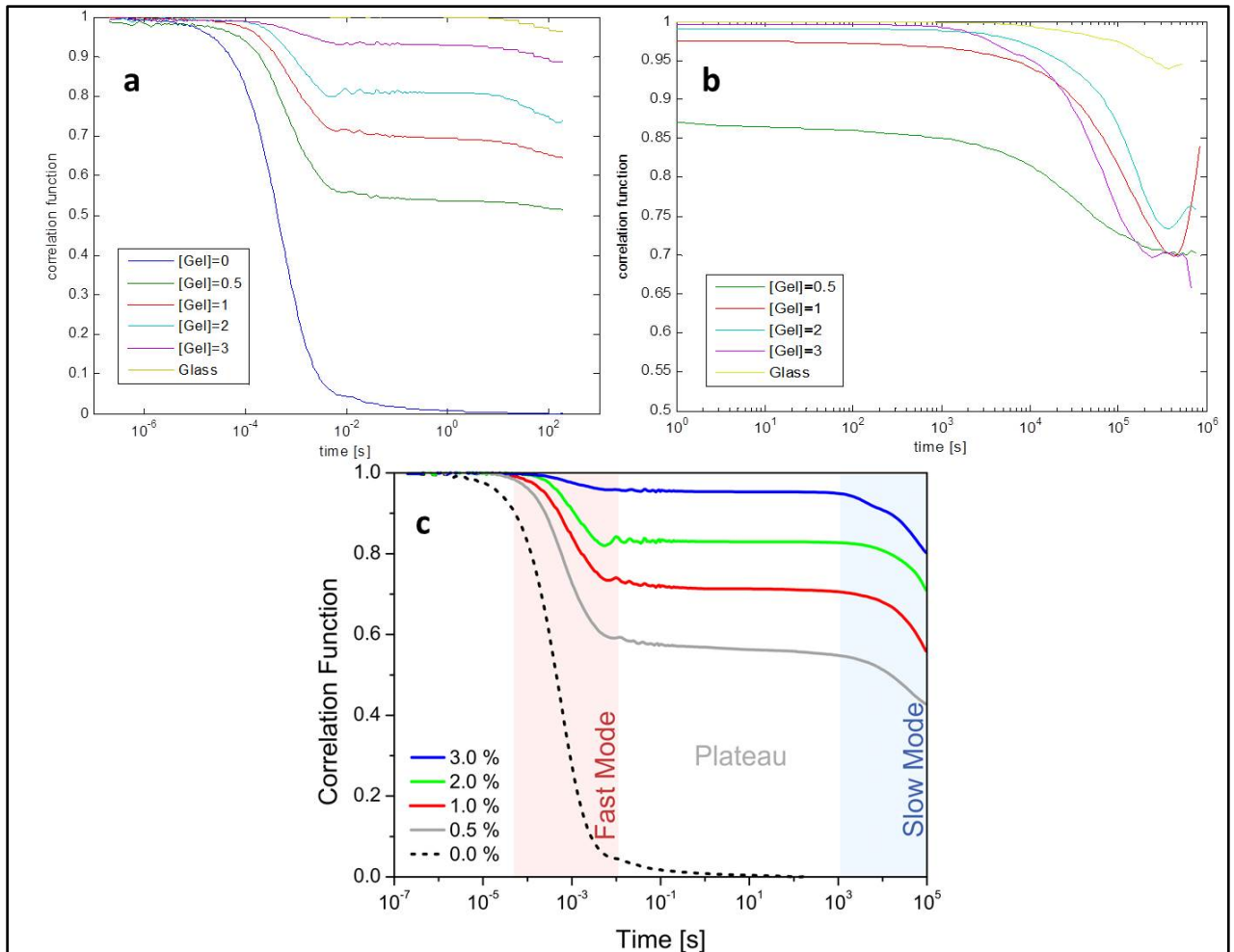
Figure 23: treatment and combination of Brute Force correlation functions with Multispeckle/Echo correlation functions; a: Brute Force correlation function after β normalization; b: Echo/Multispeckle correlation function; c: connected Brute Force and Multispeckle/Echo correlation function.

Results & Discussion

To test the Multispeckle method and the 3D-Echo-DLS method, the previously explained system of ISAsomes was employed. In particular the hexosomes (δ = 84) were used, because they are the most stable and easy to prepare phase. The mean size of the droplets was determined by DLS. The average hydrodynamic radius, calculated with the second cumulant, of about 145 nm is a reasonable good size for a dynamic light scattering experiment.
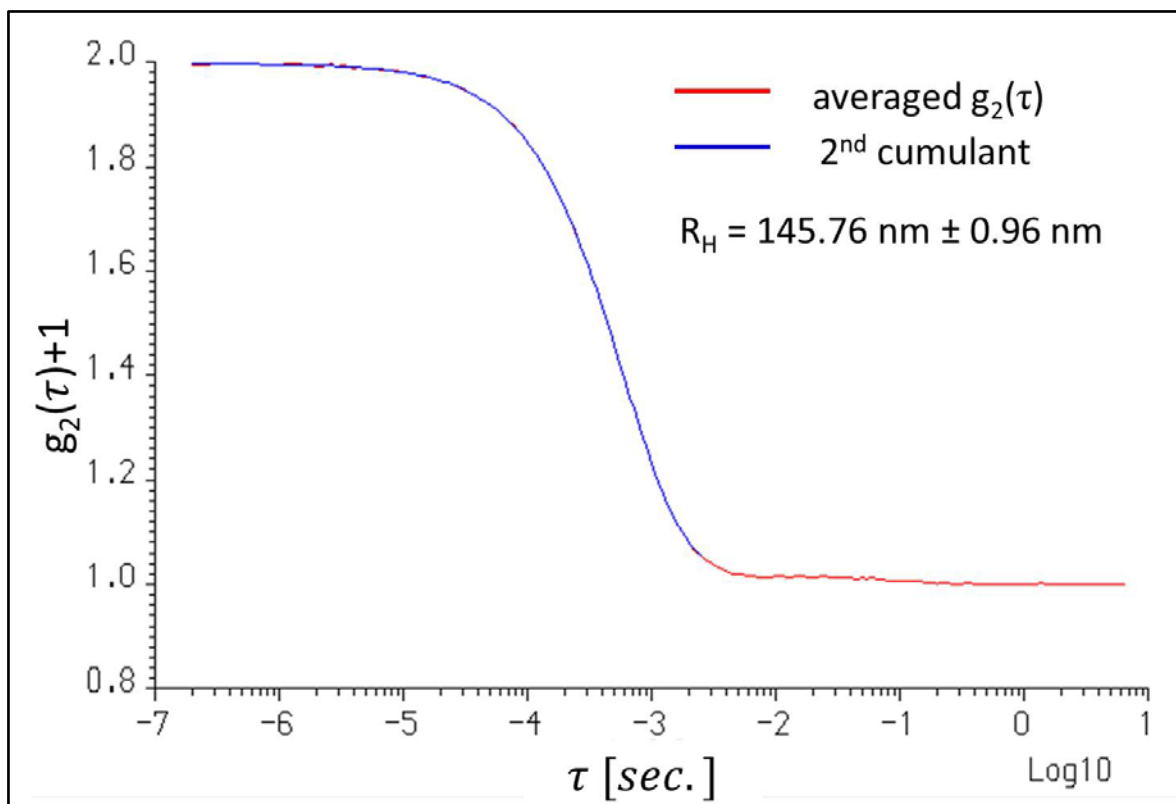
Figure 24: Exemplary DLS result of a highly diluted (4000 times) hexagonal phase (δ84)

Furthermore it was shown that KC does not have a direct influence, neither on the droplet size nor on the internal structure.[43] The used samples were also measured with SAXS (small angle x-ray spectroscopy) to show that they contain the hexagonal phase.

An example for the intact structure as well as the proof of its existence is given in Figure 25. The difference in intensity is related to the increase in the KC concentration.
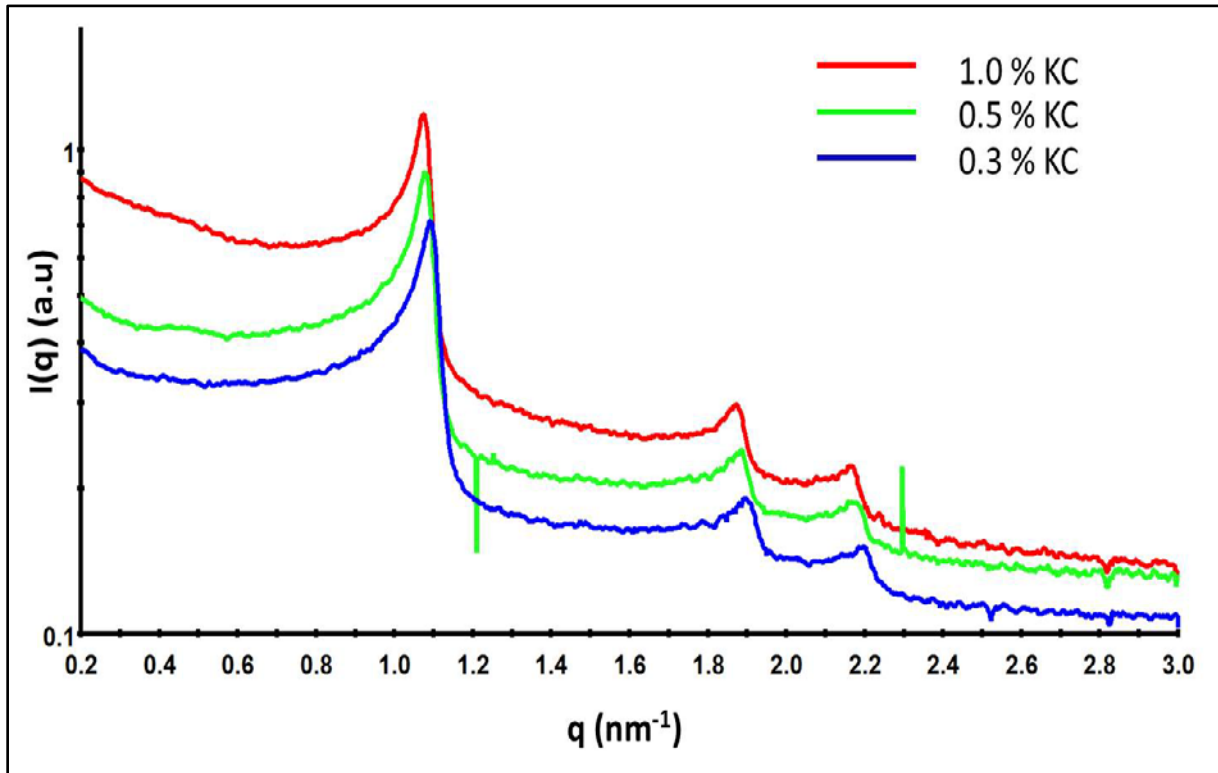

Figure 25: SAXS measurement of a hexagonal phase ($\delta 84_{\phi5}$) with 0.3 %, 0.5 % and 1.0 % KC

Effect of multiple scattering on measurement

For all experiments a flat cell of 100 µm diameter was used. As mentioned in Materials and Methods, colloidal emulsions at higher concentrations scatter light multiple times and are therefore turbid. In higher concentration regimes the amount of single scattered light becomes too low to be measured, in a 3D cross correlation technique. So the light transmittance of different concentrations of ISAsomes was measured to determine the amount of transmitted light through the flat cell. For this purpose we used the Small Angle Light Scattering Instrument (SALSA) in a very basic way (see Materials & Methods, Light Transmittance).

Isasomes [%]	Light Transmission [%]
0.0	100,00
0.5	96,59
1.0	92,01
1.5	88,64
2.0	55,63
2.5	36,42
10	0,08
20	0,01
30	0,00

Table 2 is illustrating the effect of multiple scattering on the transmission of light through the sample. Beyond 1.5 % ISAsome concentration the transmitted light is drastically reduced. At 2.0 % concentration the transmittance has dropped to half of the original signal where it is not possible any more to get good statistics in dynamic light scattering measurements. In standard experiments a light transmission of 90 % or above is required for a reasonable good signal.
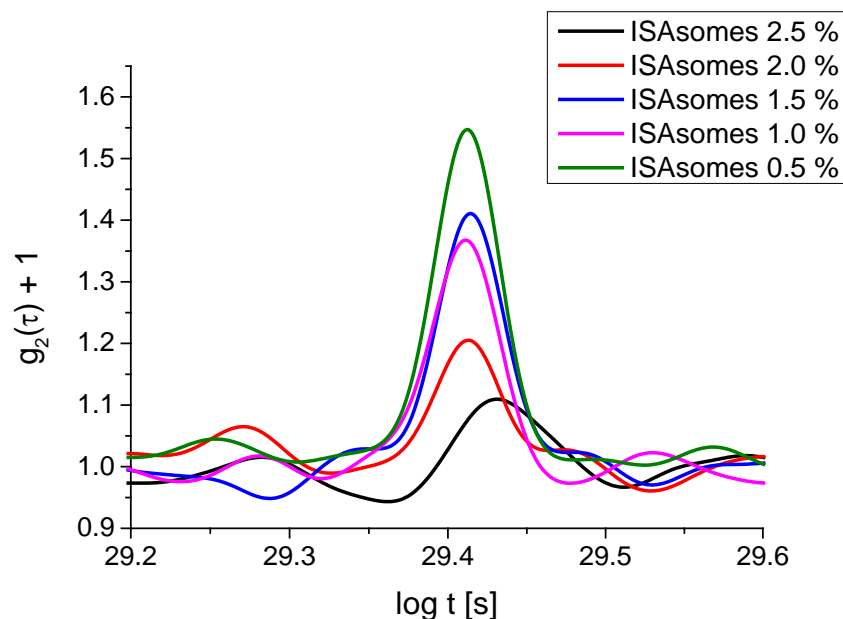

Figure 26: First Echo of the arrested system with 1 % KC at different ISAsome concentrations

Complementary to Table 2, Figure 26 shows how the echo signal vanishes with higher concentrations of ISAsomes.

Since the maximum of the echo signals are the points of the correlation function, Figure 27 shows the influence of different ISAsome concentrations on the correlation function.

We should not forget that in a 3D technique only single scattered light contributes to the signal and at higher ISAsome concentrations we have primarily multiple scattered light registered by the photomultipliers.
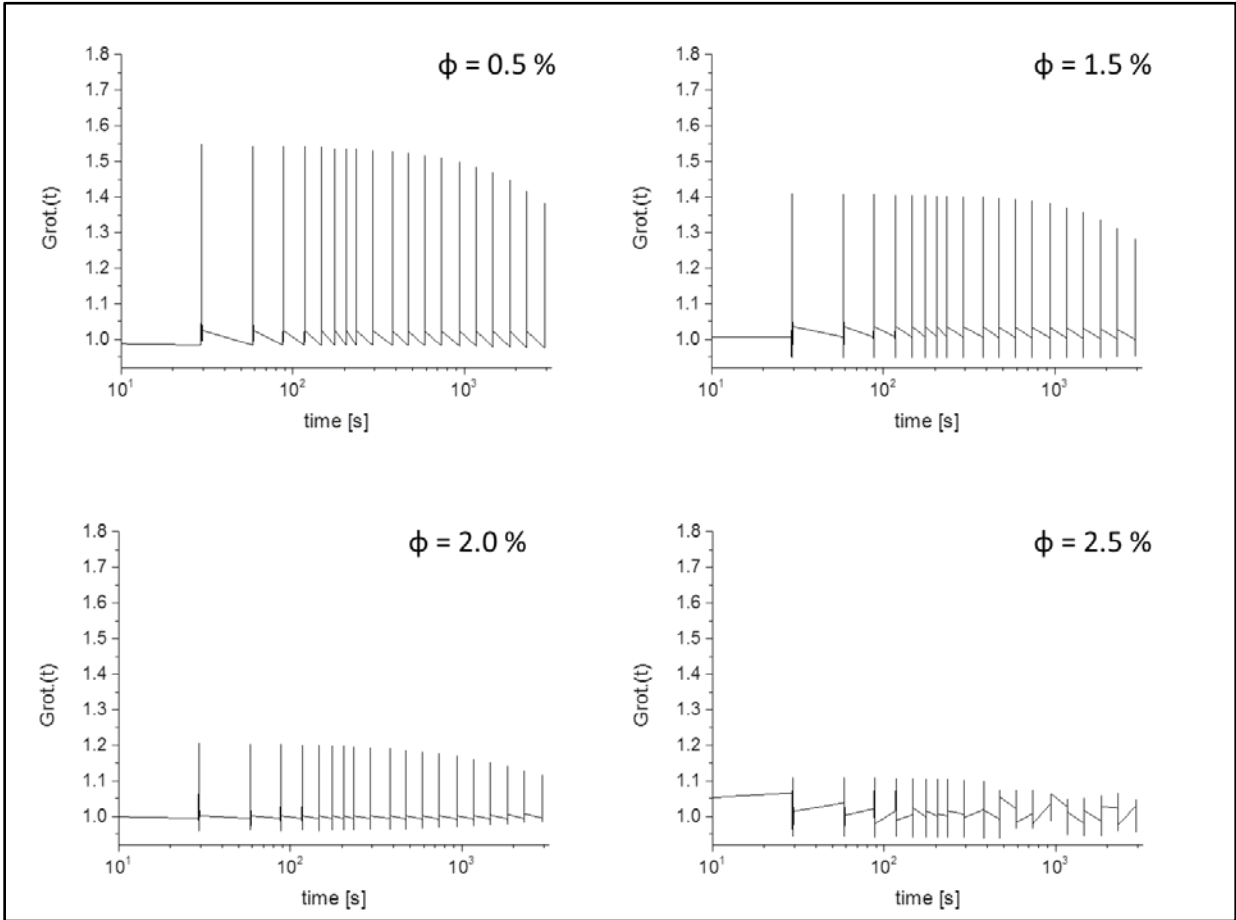

Figure 27: Influence of the ISAsome concentration (φ=0.5 %, 1.5 %, 2.0 % and 2.5 %) on the correlation function, KC concentration 1% for all; cell thickness = 100 μm

Though the effect of multiple scattering lowers the strength of the signal significantly at rather low concentrations, it would be possible to measure at higher concentrations by decreasing the thickness of the flat cell.

Depending on the size of the particles it is dangerous to decrease the cell thickness to very low values (≤ 13 μm) because wall effects can occur [40] (see Figure 28).
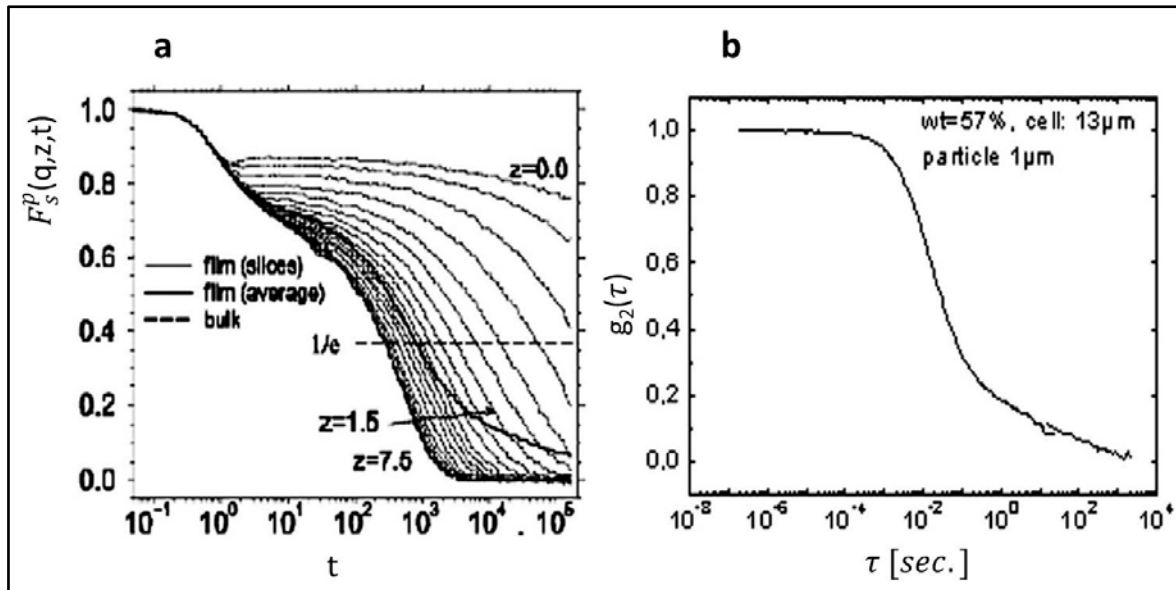

Figure 28: Depiction of the wall effect; graphs taken from Medebach et.al. [40]; Graph a: dependence of the dynamics as a function of the distance (z) from the wall, the full lines portray the scattering functions averaged over the cell thickness F_s^p(q,z,t);   b: result of Echo DLS with flat cell, the significant tail of the wall effect is visible.

Effect of Ergodicity

The 3D-Echo DLS is predestined to investigate turbid samples in a nonergodic state. Turbid, ergodic samples can be investigated, by only using the 3D cross correlation.

It is important to know how ergodic or nonergodic a sample is. The 3D-Echo DLS coupled with the Brute Force technique is capable of showing the state of ergodicity in a sample. In other words, one can see how partially arrested or diffusive the particles are in the sample. This is of course only valid for homogeneous samples.

Since we want to investigate samples with an ISAsome concentration beyond 1.5 w%, the 3D Echo method was not applicable in this case (see Results & Discussion - Effect of Multiple Scattering). Instead we investigated a sample with 5w% ISAsomes using the Multispeckle method. We increased the KC concentration at constant ISAsome concentration to show the gradual change from an ergodic to a nonergodic state (see Figure 29).
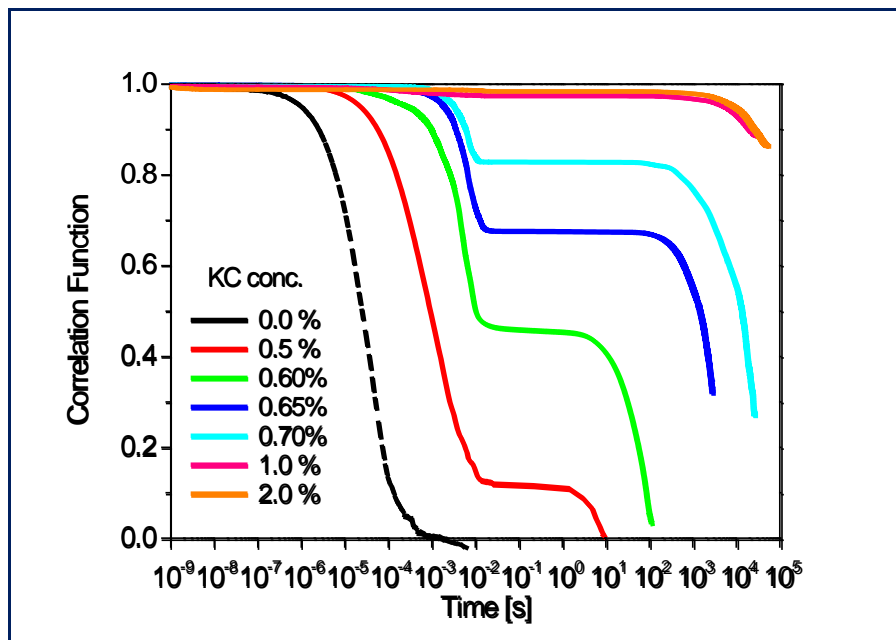

Figure 29: Determining the ergodicity of different KC concentrations using an ISAsome emulsion (φ = 5%)

As shown in Figure 29, with increasing the content of KC the viscosity of the sample is increased. The rise of the plateau marks the increasing nonergodicity. The height

of the plateau is called the nonergodicity parameter and provides information about the percentage of fixed scattering centers. Macroscopically the sample appears to be fully arrested (the sample does not flow) already at 0.5 %. In reality there is still diffusion happening, which is called "rattling in the cage" by the glass community. The KC is forming a three dimensional network throughout the sample. Therefore it is clear that the lower the concentration of gel in the sample, the bigger the mesh size. This is illustrated in Figure 30. In a rather large mesh, one small particle, or more, can easily move around, leading to the rattling. After some time the particle may even escape from the cage (final decay of the correlation function). The smaller the mesh gets, the harder it is for the particle to diffuse. When the rattling reaches a standstill it is called fully arrested dynamics (KC concentration ≥ 1 %). This means that at least on a significant timescale, no diffusion can be measured. In Figure 29 it is 10^4 seconds, where it is probable that the decrease at the end is due to instrumental imperfections. For further details see also Iglesias et al. (2014)[44] and appendix.
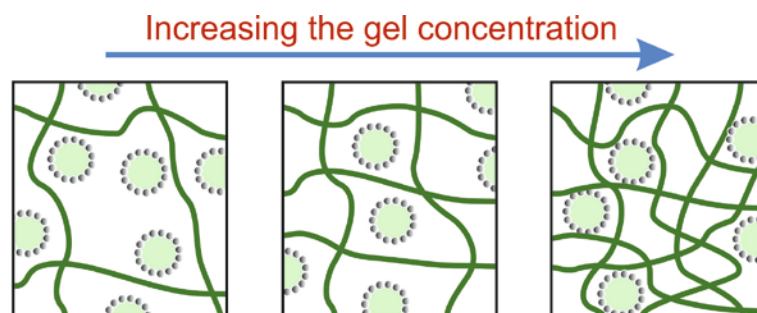

Figure 30: schematic presentation of the „cage"

The nonergodic system of glasses is well described in the works of U.Bengtzelius et al.[45], W.Götze et al.[46] and W.v.Megen et al.[47]

Conclusion

Both methods provide a good possibility to investigate the dynamics of samples in different ergodic states on a reasonable large timescale (-Echo DLS up to 10^4 s and Multispeckle up to 10^5 s).

The combination of Brute Force with either method has the benefit of showing the whole correlation time range (10^{-7} s – 10^4 s). This way it is possible to measure the transition of an ergodic state to a nonergodic state. In our case it was possible to determine the concentration of gel (KC) necessary to arrest the system over a sufficiently long period of time (- no diffusive motion).

The main problem in measuring with 3D Echo technique is the limitation on the concentration. The sample has to have a rather low concentration (see Table 2) so the amount of single scattered light is sufficient to give an evaluable signal. At higher concentrations the scattered light consists primarily of multiple scattered light.

In the Multispeckle technique we find the inverse problem. It is possible to measure higher concentrations (10 w% ISAsomes) but at lower ISAsome concentrations the recorded signal is too weak to be evaluated.

Due to this contrary limitation concerning the concentration of ISAsomes (or turbidity) it was not possible to compare the two methods with each other.

Furthermore it has to be stated that the Multispeckle measurement is of course affected by multiple scattering, even in the 100 µm cells!

To learn about the influence of multiple scattering it would be necessary to measure identical samples with both techniques.

Outlook

In our setup and used sample system it was not possible to compare both methods due to the concentration limitation.

There are basically two ways to make a comparison possible. One is to increase the ISAsome concentration in 3D Echo DLS by reducing the thickness of the flat cell. Therefore the multiple scattering will be decreased to a level so that the amount of single scattered light is sufficient for evaluation at higher sample concentrations. However in this case it is obvious that the wall effect can affect the measurement.

The other is to use lower concentrations in the Multispeckle method by increasing the signal strength. This could be done by increasing the laser power. Since our group moved in a new laboratory in the first half of 2014, new possibilities arose. Now that the Multispeckle instrument and our green diode pumped laser (see Dynamic Light Scattering) with a power range of 0.1 W to 5 W are in the same room we have the possibility to enhance the laser power for the multispeckle instrument. This will be done by guiding the laser beam into the "black box" (see Multispeckle Device - System) and through the sample via two mirrors.

Figures

References

1.   Everett, D. H. *Basic Principles of Colloid Science*. (The Royal Society of Chemistry, 1988).

2.   Bancroft, W. The Theory of Emulsification, IV. *J. Phys. Chem.* **7,** (1912).

3.   Bancroft, W. The theory of emulsification, V. *J. Phys. Chem.* **3,** (1913).

4.   Griffin, W. Classification of surface-active agents by" HLB." *J Soc Cosmet. Chem.* 311–326 (1946). at <http://ci.nii.ac.jp/naid/10004943329/>

5.   Yaghmur, A., Campo, L. De & Sagalowicz, L. Emulsified microemulsions and oil-containing liquid crystalline phases. *Langmuir* 569–577 (2005). at <http://pubs.acs.org/doi/abs/10.1021/la0482711>

6.   Engelskirchen, S. *et al.* Emulsified Microemulsion as Solvent-free Carrier for an Amorphous Solid Plant Protection Agent. *Chem. Lett.* **41,** 1125–1127 (2012).

7.   Engelskirchen, S., Maurer, R. & Levy, T. Highly concentrated emulsified microemulsions as solvent-free plant protection formulations. *J. colloid …* (2012). at <http://www.sciencedirect.com/science/article/pii/S0021979712007709>

8.   Milošević, I. *et al.* Loading and release of internally self-assembled emulsions embedded in a magnetic hydrogel. *Appl. Phys. Lett.* **104,** 043701 (2014).

9.   Chemelli, A., Maurer, M., Geier, R. & Glatter, O. Optimized loading and sustained release of hydrophilic proteins from internally nanostructured particles. *Langmuir* **28,** 16788–16797 (2012).

10.   Moitzi, C., Guillot, S., Fritz, G., Salentinig, S. & Glatter, O. Phase Reorganization in Self-Assembled Systems Through Interparticle Material Transfer. *Adv. Mater.* **19,** 1352–1358 (2007).

11.   Voorhees, P. The theory of Ostwald ripening. *J. Stat. Phys.* **38,** (1985).

12.   Urban, C. & Schurtenberger, P. Characterization of Turbid Colloidal Suspensions Using Light Scattering Techniques Combined with Cross-Correlation Methods. *J. Colloid Interface Sci.* **207,** 150–158 (1998).

13.   Stieber, F. & Richtering, W. Fiber-optic-dynamic-light-scattering and two-color-cross-correlation studies of turbid, concentrated, sterically stabilized polystyrene latex. *Langmuir* **101,** 4724–4727 (1995).

14.   Weitz, D. a, Zhu, J. X., Durian, D. J., Gang, H. & Pine, D. J. Diffusing-wave spectroscopy: The technique and some applications. *Phys. Scr.* **T49B,** 610–621 (1993).

15.   Tyndall, J. On the Blue Colour of the Sky , the Polarization of Skylight , and on the Polarization of Light by Cloudy Matter Generally Author (s): John Tyndall Source : Proceedings of the Royal Society of London , Vol . 17 (1868 - 1869), pp . 223-233 Published by. *Proc. R. Soc. London* **17,** 223–233 (1869).

16. Lorenz, L. Lysbevaegelsen i og uden for en af plane Lysbolger belyst Kugle. *Det K. Danske Vidensk. Selsk. Skr.* **6,** 1–61 (1890).

17. Mie, G. Beiträge zur Optik trüber Medien, speziell kolloidaler Metallösungen. *Ann. Phys.* **Vierte Fol,** 377–445 (1908).

18. A Brief History of Lasers. 1–8 (1950). at <http://www.kigre.com/files/historylasers.pdf>

19. Lindner, P. & Zemb, T. *Neutron, X-Ray and Light Scattering: Introduction to an Investigative Tool for Colloidal and Polymeric Systems.* (North-Holland, 1990).

20. Glatter, O. A new method for the evaluation of small-angle scattering data. *J. Appl. Crystallogr.* 415–421 (1977)

21. Brunner-Popela, J. & Glatter, O. Small-angle scattering of interacting particles. I. Basic principles of a global evaluation technique. *J. Appl. Crystallogr.* 431–442 (1997)

22. Weyerich, B., Brunner-Popela, J. & Glatter, O. Small-angle scattering of interacting particles. II. Generalized indirect Fourier transformation under consideration of the effective structure factor for polydisperse systems. *J. Appl. Crystallogr.* **32,** 197–209 (1999).

23. Bergmann, A., Fritz, G. & Glatter, O. Solving the generalized indirect Fourier transformation (GIFT) by Boltzmann simplex simulated annealing (BSSA). *J. Appl. Crystallogr.* (2000)

24. Fritz, G., Bergmann, a. & Glatter, O. Evaluation of small-angle scattering data of charged particles using the generalized indirect Fourier transformation technique. *J. Chem. Phys.* **113,** 9733 (2000).

25. Innerlohinger, J., Wyss, H. & Glatter, O. Colloidal systems with attractive interactions: Evaluation of scattering data using the generalized indirect Fourier transformation method. *J. Phys.* 18149–18157 (2004)

26. Frühwirth, T., Fritz, G., Freiberger, N. & Glatter, O. Structure and order in lamellar phases determined by small-angle scattering. *J. Appl. Crystallogr.* **37,** 703–710 (2004).

27. Guillot, S. *et al.* Direct and indirect thermal transitions from hexosomes to emulsified micro-emulsions in oil-loaded monoglyceride-based particles. *Colloids Surfaces A Physicochem. Eng. Asp.* **291,** 78–84 (2006).

28. Freiberger, N. & Glatter, O. Small-angle scattering from hexagonal liquid crystals. *J. Phys. Chem. B* **110,** 14719–27 (2006).

29. Schnablegger, H. & Glatter, O. Optical sizing of small colloidal particles: an optimized regularization technique. *Appl. Opt.* **30,** 4889–96 (1991).

30. Freiberger, N. Structural and Dynamical Characterisation of Concentrated Colloidal Systems. PhD Thesis, University of Graz (2007).

31. Pham, K. N., Egelhaaf, S. U., Moussaïd, a. & Pusey, P. N. Ensemble-averaging in dynamic light scattering by an echo technique. *Rev. Sci. Instrum.* **75,** 2419 (2004).

32.   Pham, K. Glasses in colloid-polymer mixtures. (2003).

33.   Magatti, D. & Ferri, F. Fast Multi-Tau Real-Time Software Correlator for Dynamic Light Scattering. *Appl. Opt.* **40,** 4011 (2001).

34.   Schätzel, K. Correlation techniques in dynamic light scattering. *Appl. Phys. B* **42,** 193–213 (1987).

35.   Bandyopadhyay, R., Gittings, a. S., Suh, S. S., Dixon, P. K. & Durian, D. J. Speckle-visibility spectroscopy: A tool to study time-varying dynamics. *Rev. Sci. Instrum.* **76,** 093110 (2005).

36.   De Campo, L. *et al.* Reversible phase transitions in emulsified nanostructured lipid systems. *Langmuir* **20,** 5254–61 (2004).

37.   Lehner, D., Kellner, G., Schnablegger, H. & Glatter, O. Static Light Scattering on Dense Colloidal Systems: New Instrumentation and Experimental Results. *J. Colloid Interface Sci.* **201,** 34–47 (1998).

38.   Koppel, D. E. Analysis of macromolecular polydispersity in intensity correlation spectroscopy: the method of cumulants. *J. Chem. Phys.* 4814–4820 (1972).

39.   Multispeckle-DLS Operating Manual. University of Technology Graz (2013).

40.   Medebach, M., Freiberger, N. & Glatter, O. Dynamic light scattering in turbid nonergodic media. *Rev. Sci. Instrum.* **79,** 073907 (2008).

41.   Glatter, O. *Scattering Methods, lecture notes. Lect. notes* University of Technology Graz (2014).

42.   3DDLS Spectrometer: Operation Manual. University of Technology Graz (2010).

43.   Tomsic, M., Guillot, S., Sagalowicz, L., Leser, M. E. & Glatter, O. Internally self-assembled thermoreversible gelling emulsions: ISAsomes in methylcellulose, kappa-carrageenan, and mixed hydrogels. *Langmuir* **25,** 9525–34 (2009).

44.   Iglesias, G. R., Pirolt, F., Tomšič, M. & Glatter, O. Dynamics of liquid-crystalline emulsion droplets arrested in hydrogels: Addressing the multiple scattering problem in turbid systems. *Colloids Surfaces A Physicochem. Eng. Asp.* 6–11 (2014). doi:10.1016/j.colsurfa.2014.11.047

45.   Bengtzelius, U., Götze, W. & Sjölander, A. Dynamics of supercooled liquids and the glass transition. *J. Phys. C* **5915,** (1984).

46.   Götze, W. & Sjogren, L. Relaxation processes in supercooled liquids. *Reports Prog. Phys.* **241,** (1992).

47.   Megen, W. Van & Underwood, S. Glass transition in colloidal hard spheres: Measurement and mode-coupling-theory analysis of the coherent intermediate scattering function. *Phys. Rev. E* **49,** 4206–4220 (1994).
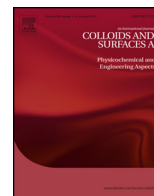
Appendix

Dynamics of liquid-crystalline emulsion droplets arrested in hydrogels: Addressing the multiple scattering problem in turbid systems

Guillermo Ramon Iglesias [a,b], Franz Pirolt [b], Matija Tomšič [c], Otto Glatter [b,*]

[a] *Department of Applied Physics, School of Science, University of Granada, 18071 Granada, Spain*
[b] *Department of Chemistry, Karl-Franzens-University Graz, Heinrichstraße 28, 8010 Graz, Austria*
[c] *University of Ljubljana, Faculty of Chemistry and Chemical Technology, Večna pot 113, 1000 Ljubljana, Slovenia*

HIGHLIGHTS

- DLS instrument with multispeckle detector and brute force detection is described.
- A series of DLS results for turbid colloidal suspensions are presented.
- Diffusion of lipid droplets entrapped in polymeric hydrogels is studied.
- Polymer concentration necessary to arrest lipid droplets is determined.

GRAPHICAL ABSTRACT
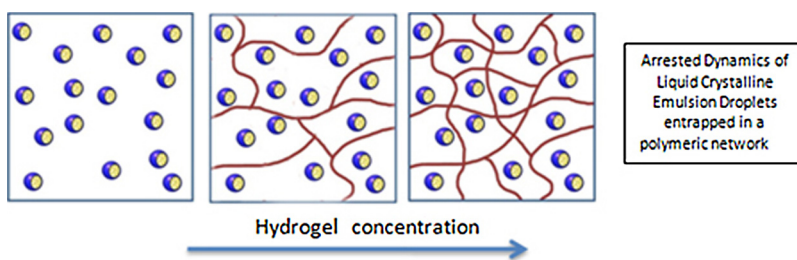
ARTICLE INFO

ABSTRACT

Performing dynamic light scattering (DLS) measurements on turbid samples is still a great challenge. A standard DLS instrument will provide reliable measurements as long as the sample is transparent and ergodic. Measurements on highly concentrated systems, on the other hand, such as glasses or gels, show partially frozen dynamics or incomplete relaxation processes. Such systems are called nonergodic. Nonergodic systems commonly appear in various practical applications and are therefore of great scientific as well as industrial interest. Many of these systems show high turbidity caused by the multiple scattering. The contribution of multiple scattering accompanied by low light transmission often leads to false DLS results for such systems, since standard DLS theory is only valid for single-scattered light. We describe here a DLS instrument that has been modified to address this problem. We use a charge-coupled device (CCD) camera as a multispeckle detector, and combine single-mode fiber optics with a photomultiplier to determine both ensemble and time-averaged autocorrelation functions. The instrument features a thin, flat sample cell with a translation stage. We show some DLS results for a series of turbid colloidal suspensions, where the lipid droplets are entrapped in polymeric hydrogels of different polymer concentrations. We focus on the transition from ergodicity to nonergodicity using ensemble-averaged DLS-intensity autocorrelation functions.

* Corresponding author at: Graz University of Technology, Institute of Inorganic Chemistry, Stremayrgasse 9/V, A-8010 Graz, Austria. Tel.: +43 316 873 32146/32101; fax: +43 316 873 32102.
E-mail address: otto.glatter@uni-graz.at (O. Glatter).

G Model
COLSUA-19563;   No. of Pages 6

ARTICLE IN PRESS

2   *G.R. Iglesias et al. / Colloids and Surfaces A: Physicochem. Eng. Aspects xxx (2014) xxx–xxx*

1. Introduction

Dynamic light scattering (DLS) is a well-established technique for particle sizing in dilute and transparent dispersions, but in the last few years it has seen an important development that currently allows us to probe a number of dynamic features of complex fluids and viscoelastic solids, such as colloidal glasses and gels [1,2]. This development is essentially based on charge-coupled device (CCD) sensor technology [3]. Most current applications of static light scattering (SLS) and DLS rely on experiments with samples that only exhibit single scattering, whereas industrially relevant samples often show multiple scattering. Measurements on transparent and ergodic systems can be made easily using standard light scattering techniques [4–7], because the multiple scattering in such systems is negligible. In contrast, DLS measurements become more difficult in highly concentrated colloidal systems, which can show phase transitions from fluid to solid or gel, or even to a glassy state, depending on the particle concentration and polydispersity [8–23].

Such systems are usually nonergodic, i.e., they show partially frozen dynamics and/or incomplete relaxation processes. Many of them also exhibit high turbidity (low light transmission) caused by multiple scattering, which often hinders DLS measurements and the corresponding data evaluation. The evaluation of such data in terms of general DLS theory, which is based on the assumption that every photon is scattered only once, is not reliable. Thus, a number of experimental techniques have been developed to deal with the problem of multiple scattering. Diffusing wave spectroscopy (DWS) introduced in 1987 [3,24–27] is based on multiple scattering and is therefore well-suited to very turbid samples. Two-color cross-correlation and 3-D cross-correlation techniques [18,20,23] can eliminate multiple scattering contributions, while techniques based on measurements of back-scattering [19] and the reduction of the beam's path length in the sample [9,28–32] can reduce multiple scattering to a negligible amount, as long as the optical density is not too high. The so-called "echo technique" introduced by Pham et al. [33] is well suited to nonergodic samples, and has been recently combined with a thin, flat-cell design [29].

If the concentration is high enough, the typical time scale of the dynamics of such a system can be increased by several orders of magnitude, or some modes of motion can be completely frozen. As soon as the particles move, the intensity of the speckles changes, and this intensity fluctuation is directly related to the dynamics of the particles. Thus, in a DLS experiment the intensity is measured as function of time.

In ergodic systems, for a sufficient long time of observation, all possible particle configurations are present in the measuring volume and, if the statistics of the DLS measurements are good enough, the intensity fluctuations reflect all the different states of an ensemble; in other words, time-averaged measurements fully reflect the dynamics of the system.

In a nonergodic system, some modes of motion are frozen, and the time average is no longer equal to the ensemble average; thus, the time average does not properly represent the dynamics of the system. Rather, only the intensity fluctuations of many independent speckles fully reflect the dynamics of the system. Therefore, the correct DLS correlation function is only obtained as the ensemble-averaged intensity correlation function calculated as the intensity correlation function averaged over all the speckles [34–38].

The ensemble-averaged intensity correlation function in nonergodic systems is measured by averaging over many independent speckles. One possible technique to measure such an average is the so-called "brute-force method" introduced by Pusey et al. [39–41]. In this technique, the time-averaged correlation function is measured for a fixed sample position (laser speckle); then, the sample is slightly moved (rotated or translated) and a new measurement in a new speckle is started. In this way, all correlation functions can be averaged. However, the time needed to perform the DLS measurements with high correlation times is unreasonably long. For example, to get the correlation function up to $\tau_{max} = 10^3$ s, the total time for the measurement would be around 14 days [42]. This means that the "brute-force" method can practically only be used to investigate short time dynamics of nonergodic systems (up to a few seconds).

To investigate long time dynamics in ergodic as well as nonergodic samples (typically from ~1 to 10^4 s or more) the multispeckle method (MSM) can be used, as initially shown by Kirsch et al. [43], who used a multi-pixel detector to measure slow relaxations in colloidal systems with a video camera in a traditional light scattering experiment [43–46]. The main advantage of the MSM is that the temporal evolution of the correlation function can be resolved. This makes it possible to investigate time-dependent [45,47] or heterogeneous dynamics [48].

A charge-coupled device (CCD) sensor can be useful in such systems because it is equivalent to a large ensemble of intensity detectors working simultaneously. The main limitation of such a CCD DLS scheme is related to the limited frame rate of standard CCD cameras (currently of the order of 0.1–1 kHz), which is much slower than fast hardware autocorrelators (up to 100 MHz). In order to cover the full spectrum of correlation times, the CCD multi-speckle detection needs to be combined with a traditional DLS for ergodic systems or with a brute-force measurement for nonergodic systems [46,49,50].

The aim of the present work was to measure the arrested dynamics of emulsion droplets of turbid O/W emulsions in hydrogels with varying concentrations of the gelling agent; i.e., we wanted to measure the ergodic–nonergodic transitions in these samples. In the following, we present our in-house-built instrument combining the two different methods, brute-force and MSM. In the brute-force method, we use a single-mode fiber with a photomultiplier as a detector. The sample cell can be translated vertically by a stepper motor. For slow dynamics, we added a CCD multi-pixel sensor to the goniometer arm, working as a multispeckle detector. This device can be used for correlation times from 1 to 10^4 s or more. The instrument is equipped with a thin, flat sample cell of variable thickness from approximately 13 to 500 μm, with the important condition that the glass windows of the planar sample cell are perfectly parallel to each other guaranteed by special calibrated distance rings. A similar cell has been successfully used for static and dynamic light scattering experiments [8].

2. Materials and methods

2.1. Materials

In our test experiments, we used internally self-assembled liquid-crystalline lipid emulsions, either in water or entrapped in polymeric hydrogels. The droplets consist of Dimodan® U/J (Material no. 015312 (DU), donated by DANISCO A/S, Braband, Denmark). This material is a distilled monoglyceride mixture (mostly C_{18}-chains) comprising 96% monoglycerides with 62% linoleate and 25% oleate. The second lipid component, used to tune the internal structure, was the oil tetradecane ($C_{14}H_{30}$, olefin free, purity $\geq$99.0%, Sigma–Aldrich). The triblock copolymer Pluronic® F127 (PEO_{99}–PPO_{67}–PEO_{99}, donated by BASF, USA), was chosen as the stabilizer of the emulsions. The gelling agent was κ-carrageenan (KC) (technical grade, Sigma–Aldrich). All materials were used without further purification. Milli-Q water (Millipore) was utilized as the solvent. All measurements were performed at 25 °C unless stated otherwise.
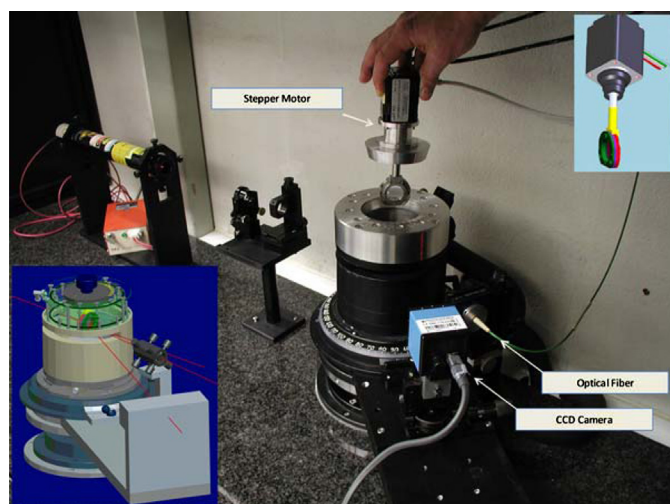
G Model
COLSUA-19563; No. of Pages 6

ARTICLE IN PRESS

G.R. Iglesias et al. / Colloids and Surfaces A: Physicochem. Eng. Aspects xxx (2014) xxx–xxx

3

Fig. 1. Photo of the multispeckle DLS instrument with all components. Left lower corner: schematic of the setup combined with a fiber optic holder and CCD chip behind the gray wall. Upper right corner: schematic of the stepper motor combined with the flat cell for the brute-force measurements.

2.2. Sample preparation

The hydrophobic component tetradecane, together with the monoglycerides, constituted the lipid phase of the system. By changing their concentration ratio in the system, it was possible to tune the internal structure of the droplets. DU forms self-assembled bicontinuous cubic phases in excess water [51]. Addition of simple oils, such as tetradecane, leads to various structures, such as hexagonal, inverse-micellar or microemulsion phases at room temperature, depending on the oil content. The phase diagram for these structures is normally presented according to the mass ratio (δ) between DU and (tetradecane + DU). The lipid phases can be dispersed in water, stabilized by F127, to form *I*nternally *S*elf-*A*ssembled particles (somes) called ISAsomes [52].

The ISAsome samples contained 10% of the dispersed phase and were prepared such that $\delta = 84\%$, leading to a reverse hexagonal H_2 phase (hexosomes). The samples were dispersed by ultrasonication (Vibra-Cell, Sonics & Materials, Newtown, CT, USA) for 5 min with an amplitude of 30% (pulse 0.5 s; break 1.5 s) leading to particle diameters of about 200 nm. The emulsion particles were entrapped by using an aqueous solution of the gelling polymer κ-carrageenan prepared at high temperature (65 °C). Aqueous dispersions of κ-carrageenan are known to undergo reversible sol/gel transitions with changes in temperature [53]. A gel forms at ambient temperature, becoming fluid above approximately 50 °C. ISAsome/gel mixtures were prepared by blending equal amounts of ISAsome solutions with κ-carrageenan/water mixtures [54] to reach final concentrations of 0.50%, 0.60%, 0.65%, 0.70%, 0.75%, 1.0% and 2.0% for the gelling agent and 5% ISAsomes. The blending and filling processes were carried out at 55 °C to ensure a fluid state and homogeneous mixing of the system. The sample was poured into the flat light-scattering cell with a thickness of 100 μm. The cell was placed in an ice-water bath for 5 min for rapid cooling and gelation, and was then equilibrated for 1 min in a water bath (25 °C) before being transferred into the thermostat-controlled cell holder (25 °C). The time from the initial mixing to the start of measurements was 10 min.

2.3. DLS: the flat-cell multispeckle instrument

Our flat-cell multispeckle DLS instrument is a laboratory-built goniometer, equipped with a 10 mW HeNe laser, λ = 632.8 nm (NEC

Fig. 2. Flat sample-cell. Top: schematic view. The cell consists of two main parts (red and green) with glued-in glass windows (optical flats, dark blue) and o-ring sealing. The sample thickness is controlled by the middle spacer ring (pink). The cell is connected to the stepper motor by the yellow shaft. Bottom left: section view; bottom right: front view, assembled.

Corp., GFO Germany), single-mode fiber detection (OZ from GMP, Switzerland), an ALV/SO-SIPD/DUAL photomultiplier with pseudo-cross-correlation option, and an ALV 5000/E correlator with fast expansion (ALV, Germany). A CCD camera, as a second detector, is placed on the same goniometer arm as the fiber, but at an offset of 15°. The CCD camera (Sony DMK 21BU04) has a resolution of 640 × 480 pixels, and a pixel size of 5.6 μm × 5.6 μm at a distance of 180 mm from the sample. The schematic drawing and a photo of the instrument are shown in Fig. 1. The sample holder is thermostated to maintain constant temperature for the duration of the investigation.

2.4. Flat sample-cell design

One approach to the problem of multiple scattering is to reduce the light path through the sample. For this purpose, we developed a flat sample cell whose thickness can be tuned from around 13 to 500 μm with different calibrated distance rings [29]. Reducing the thickness increases the transmission and reduces (but does not completely remove) the amount of multiple scattering. In this work, we used a sample thickness of 100 μm. Fig. 2 shows the detail of the cell design and the calibrated spacer ring. Diffusing wave spectroscopy (DWS) [26] is not suitable in this case, because it relies on strong multiple scattering.

2.5. DLS: short-term measurements (brute-force)

The ensemble-averaged intensity correlation function for times of less than 1 s in nonergodic systems is measured by averaging many independent speckles [55,56]. Due to the limitations of the CCD camera (read-out rate ≤1 picture/s) it could not be used to perform such fast measurements. For this purpose, we used the so-called "brute-force" method with an optical single-mode fiber and photomultiplier detection [39–41,57]. The main difference between our method and that used by Pham et al. [33] and Medebach et al. [8] is that we cannot rotate the flat cell in our setup, but we can move it vertically by using a programmable stepper motor and a linear actuator (Haydon Kerk Motion Solutions, Waterbury, USA), which is operated by 12 V DC input voltage and used to

G Model
COLSUA-19563; No. of Pages 6

ARTICLE IN PRESS

4 *G.R. Iglesias et al. / Colloids and Surfaces A: Physicochem. Eng. Aspects xxx (2014) xxx–xxx*

move the cell vertically step-by-step (user-selectable step width). The scattered light was detected by a photomultiplier via single-mode fiber-detection optics (OZ from GMP, Zurich, Switzerland). Data were analyzed by using an ALV5000/E correlator (ALV, Langen, Germany).

The basic principle of the proposed method is to measure the intensity correlation function for a large series of independent speckles. In the first step, the sample is fixed, the intensity fluctuation of one speckle is then measured (speckle no. 1, distance $d = 0$), and the time-averaged intensity correlation function is calculated. The sample is then shifted up by distance Δd to position $d + \Delta d$ to measure the intensity correlation function of speckle no. 2. This procedure is repeated many times to get a reliable ensemble-averaged correlation function. In our setup, the stepper motor is mounted on top of the goniometer (Fig. 1) to allow vertical scanning of the sample with a measuring time $t = 600$ s for each position. The sample is moved up step-wise by $\Delta d = (3.2 \pm 0.2)\,\mu$m and another data set is taken automatically. The complete scanning regime is in the order of several millimeters. The resulting 80 correlation functions are averaged to obtain the ensemble-averaged short-term correlation function. The maximum correlation time obtained for the 600 s measurements is about 30 s. This method gives an intercept close to one for the correlation function of ergodic systems. The corresponding imperfections of the instrument are eliminated by a factor normalizing the correlation function to unity at zero delay time. These brute-force measurements facilitate the determination of the correlation functions in the time interval from 10^{-7} to 30 s.

2.6. Long-term measurement (multispeckle detection)

The CCD camera is connected to a PC and records the speckle pattern (640×480 pixels) at a fixed, user-selectable time with a maximum rate of 1 picture per second. The pixel size of the camera does not automatically correspond to the speckle size, the latter depending on the optical set-up. In any case, the pixels must not be larger than the speckles. If the speckle size is about n times greater than the pixel size it is advisable to average over $n \times n$ pixels to create an "averaged" pixel intensity I_{pixel}, in our case ($n = 3$) of 3×3 pixels. After data acquisition, we examine the evolution of the intensity autocorrelation function $g_2(\tau)$ over time [45].

The function $g_2(\tau) - 1 = c_I(t, \tau)$ is calculated for a set of fixed lag times τ and for a given and fixed wave vector q [58]:

$$g_2(\tau) - 1 = \langle c_I(t, \tau) \rangle_{time} = \left\langle \frac{\langle I_{pixel}(t) I_{pixel}(t + \tau) \rangle_{pixel}}{\langle I_{pixel}(t) \rangle_{pixel} \langle I_{pixel}(t + \tau) \rangle_{pixel}} - 1 \right\rangle_{time}$$

where I_{pixel} denotes the intensity at an "averaged" pixel and τ is the lag time between two pictures while $\langle \cdots \rangle_{pixel}$ the average over all the "averaged" pixels of the CCD image corresponding to a given q value. It is possible to detect intermittent behavior in the $c_I(t, \tau)$ signal by examining the variation around its mean for different lag times [58], in order to obtain information about the dynamics of intermediate or slow diffusion of the droplets. The patterns were accumulated every 30 s for more than 25 h to obtain this information. The resulting curves show the changes in correlation functions at the time range, in our setup, from 30 to 10^5 s. Note that these curves were normalized by a constant, so that at the time of 30 s, the value of the correlation function is the same as that obtained from the corresponding short-term measurement (the end point of the curve from short-term diffusion dynamics). In order to obtain the complete ensemble-averaged correlation function, a merge of the short- and long-term correlation functions is performed.
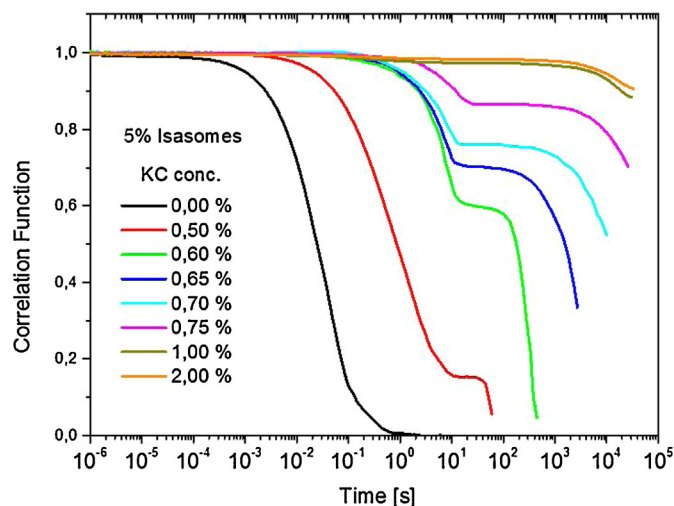

Fig. 3. Correlation functions combined from brute-force and multispeckle DLS data for samples of 5% ISAsomes loaded into varying concentrations of κ-carrageenan gels. A flat-cell with thickness of 100 μm and scattering angle of 30° was used.

3. Results and discussion

3.1. Ergodic to nonergodic transition

In this study, we investigated the arrested diffusion dynamics of the ISAsome O/W emulsions embedded in a polymeric network that turns the system from ergodic to nonergodic. For this purpose, we used the κ-carrageenan (KC) hydrogel, which is transparent and does not increase the turbidity of the emulsions. The diffusion of emulsion droplets can be arrested by their incorporation into such network structures [59,60].

The dynamics of the droplets embedded in a gel at various concentrations of the gelling polymer was evaluated by using the autocorrelation function obtained from the combined "brute-force" and multispeckle DLS data, as shown in Fig. 3. Note that these DLS data are not completely free from multiple scattering contributions, due to the strong scattering power of the emulsion droplets. On the other hand, the κ-carrageenan hydrogel is transparent and has a negligible scattering power compared to the emulsion. So, any changes in the measured correlation function as a function of hydrogel content cannot be attributed to the effect of multiple scattering. The brute-force DLS measures the fast dynamics of motion (for decay times between 10^{-7} and 30 s), and requires many repetitions at different sample positions to get the ensemble average for nonergodic media. Multispeckle data provide information on the slow-motion dynamics (10^1–10^5 s) in one run, as many speckles can be measured simultaneously. These combined curves are presented in Fig. 3.

According to Fig. 3, the correlation function shows two sections or modes (fast and slow), the plateau between them representing the "frozen" (nonergodic) state. The fast mode slows down from about 10^{-2} to 10^1 s as KC is added, increasing the polymer concentration. At the same time, its relative amplitude decreases dramatically above 0.5% KC, where the sample turns from a viscous fluid to a gelled system (around 0.7% KC) and the correlation function starts to show a plateau of increasing length (≥ 2 orders of magnitude). In this regime, the fast mode can be understood as "rattling in the cage": the ISAsome droplet motion is limited by the pore size of the gel, and the system is nearly arrested. Eventually, the droplets start to escape from the cage, leading to the second slow mode in the dynamic response of the system. As the concentration of KC is increased to 1% or more, the plateau level is close to one. At this point, the system is nearly completely frozen and there

G Model
COLSUA-19563; No. of Pages 6

ARTICLE IN PRESS

G.R. Iglesias et al. / Colloids and Surfaces A: Physicochem. Eng. Aspects xxx (2014) xxx–xxx

5

is no escape from the pores, at least not in the time frame of 10^4 s (several hours). In this case, the size of the cages in the hydrogel is smaller or comparable to the size of the ISAsomes.

We used a sample cell of thickness of 100 μm in the experiments in order to avoid possible wall effects on the dynamics of the system [29]. At the same time, the effect of multiple scattering is highly reduced, but not negligible. It is not trivial to estimate these effects. However, when comparing different samples with the same fixed emulsion concentration but different amounts of gelling agent, we know that these remaining multiple scattering effects are identical for all samples, because the scattering power of the transparent polymer gel is perfectly negligible.

A potential solution to this problem might have been to use the 3D-echo setup we developed recently [29]. Nonetheless, under our experimental conditions, the echoes disappeared quickly and a comparison with MSM data was not possible. Although the situation improved when the oil concentration (and turbidity) was reduced, the sensitivity of our CCD system was not high enough at the given laser power in these dilute systems. We plan to compare the 3D-echo setup and the multispeckle CCD instrument using a high-power laser in future work. Such data could then also be compared with results from DWS.

4. Conclusion

In this contribution, we describe a modification of conventional dynamic light scattering (DLS) instrument based on using a charge-coupled device (CCD) camera as multispeckle detector and single-mode fiber optics combined with a photomultiplier in order to measure nonergodic and turbid systems. The setup described, utilizing the thin flat cell on a translation stage, provides a useful method to measure the transition to nonergodic conditions at medium turbidity. In our example of an O/W emulsion embedded in a hydrogel, we showed that it is possible to determine the polymer concentration necessary to arrest the diffusion motion of the droplets.

Acknowledgments

References

[1] F. Scheffold, P. Schurtenberger, Light scattering probes of viscoelastic fluids and solids, Soft Materials 1 (2003) 139–165.

[2] C. Moitzi, R. Vavrin, S.K. Bhat, A. Stradner, P. Schurtenberger, A new instrument for time-resolved static and dynamic light-scattering experiments in turbid media, J. Colloid Interface Sci. 336 (2009) 565–574.

[3] F. Scheffold, R. Cerbino, New trends in light scattering, Curr. Opin. Colloid Interface Sci. 12 (2007) 50–57.

[4] R. Pecora, Dynamic light-scattering from polymers, Makromol. Chem. Macromol. Chem. Phys. (1979) 73–80.

[5] R. Pecora, Dynamic light scattering measurement of nanometer particles in liquids, J. Nanopart. Res. 2 (2000) 123–131.

[6] P. Zakharov, F. Scheffold, Advances in dynamic light scattering techniques, in: Light Scattering Reviews 4: Single Light Scattering and Radioactive Transfer, Springer-Praxis Publishing Ltd., Chichester, UK, 2009, pp. 433–467.

[7] F. Fankhauser II, Application of static and dynamic light scattering – a review, Klin. Monatsbl. Augenheilkd. 227 (2010) 194–198.

[8] M. Medebach, M. Dulle, O. Glatter, Slow dynamics in dense oil–water emulsions studied using dynamic light scattering, J. Phys. Condens. Matter 21 (2009) 504111.

[9] M. Medebach, C. Moitzi, N. Freiberger, O. Glatter, Dynamic light scattering in turbid colloidal dispersions: a comparison between the modified

[10] flat-cell light-scattering instrument and 3D dynamic light-scattering instrument, J. Colloid Interface Sci. 305 (2007) 88–93.

[10] C. Moitzi, N. Freiberger, O. Glatter, Viscoelastic wormlike micellar solutions made from nonionic surfactants: structural investigations by SANS and DLS, J. Phys. Chem. B 109 (2005) 16161–16168.

[11] A.K. Sood, Structural ordering in colloidal suspensions, Solid State Phys. Adv. Res. Appl. 45 (1991) 1–73.

[12] H. Lowen, Melting, freezing and colloidal suspensions, Phys. Rep. Rev. Sect. Phys. Lett. 237 (1994) 249–324.

[13] V.A. Martinez, G. Bryant, W. van Megen, Aging dynamics of colloidal hard sphere glasses, J. Chem. Phys. 133 (2010).

[14] W. van Megen, Dynamical perspective of the freezing transition of a suspension of hard spheres from the velocity autocorrelation function, Phys. Rev. E 73 (2006).

[15] S.R. Williams, P. McGlynn, G. Bryant, I.K. Snook, W. van Megen, Dynamical signatures of freezing: stable fluids, metastable fluids, and crystals, Phys. Rev. E 74 (2006).

[16] G. Nagele, On the dynamics and structure of charge-stabilized suspensions, Phys. Rep. Rev. Sect. Phys. Lett. 272 (1996) 216–372.

[17] P. Walstra, Estimating globule-size distribution of oil-in-water emulsions by spectroturbidimetry, J. Colloid Interface Sci. 27 (1968) 493–500.

[18] K. Schatzel, Suppression of multiple-scattering by photon cross-correlation techniques, J. Mod. Opt. 38 (1991) 1849–1865.

[19] F. Stieber, W. Richtering, Fiber-optic-dynamic-light-scattering and two-color-cross-correlation studies of turbid, concentrated, sterically stabilized polystyrene latex, Langmuir 11 (1995) 4724–4727.

[20] E. Overbeck, C. Sinn, T. Palberg, K. Schatzel, Probing dynamics of dense suspensions: three-dimensional cross-correlation technique, Colloids Surf. A: Physicochem. Eng. Asp. 122 (1997) 83–87.

[21] Y.S. Yang, H.L. Liu, X.D. Li, B. Chance, Low-cost frequency-domain photon migration instrument for tissue spectroscopy, oximetry, and imaging, Opt. Eng. 36 (1997) 1562–1569.

[22] H.B. Jiang, J. Pierce, J. Kao, E. Sevick-Muraca, Measurement of particle-size distribution and volume fraction in concentrated suspensions with photon migration techniques, Appl. Opt. 36 (1997) 3310–3318.

[23] C. Urban, P. Schurtenberger, Characterization of turbid colloidal suspensions using light scattering techniques combined with cross-correlation methods, J. Colloid Interface Sci. 207 (1998) 150–158.

[24] G. Maret, P.E. Wolf, Multiple light-scattering from disordered media – the effect of brownian-motion of scatterers, Z. Phys. B: Condens. Matter 65 (1987) 409–413.

[25] D.J. Pine, D.A. Weitz, P.M.E. Chaikin, Herbolzheimer, diffusing-wave spectroscopy, Phys. Rev. Lett. 60 (1988) 1134–1137.

[26] D.A. Weitz, D.J. Pine, D.J. Durian, J.X. Zhu, Diffusing wave spectroscopy – the dynamics of multiply scattering media, in: Symposium on Application of Multiple Scattering Theory to Materials Science, At the 1991 Fall Meeting of the Materials Research Society, Boston, MA, 1991, p. 421.

[27] D.A. Weitz, J.X. Zhu, D.J. Durian, D.J. Pine, Principles and Applications of Diffusing-Wave Spectroscopy, Springer, The Netherlands, 1992.

[28] T.W. Patapoff, T.H. Tani, M.E.M. Cromwell, A low-volume, short-path length dynamic light scattering sample cell for highly turbid suspensions, Anal. Biochem. 270 (1999) 338–340.

[29] M. Medebach, N. Freiberger, O. Glatter, Dynamic light scattering in turbid nonergodic media, Rev. Sci. Instrum. 79 (2008).

[30] J. Innerlohinger, H.M. Wyss, O. Glatter, Colloidal systems with attractive interactions: evaluation of scattering data using the generalized indirect Fourier transformation method, J. Phys. Chem. B 108 (2004) 18149–18157.

[31] D. Lehner, G. Kellner, H. Schnablegger, O. Glatter, Static light scattering on dense colloidal systems: new instrumentation and experimental results, J. Colloid Interface Sci. 201 (1998) 34–47.

[32] H. Lindner, G. Fritz, O. Glatter, Measurements on concentrated oil in water emulsions using static light scattering, J. Colloid Interface Sci. 242 (2001) 239–246.

[33] K.N. Pham, S.U. Egelhaaf, A. Moussaid, P.N. Pusey, Ensemble-averaging in dynamic light scattering by an echo technique, Rev. Sci. Instrum. 75 (2004) 2419–2431.

[34] P.N. Pusey, W. Vanmegen, Dynamic light-scattering by non-ergodic media, Physica A 157 (1989) 705–741.

[35] J.G.H. Joosten, E.T.F. Gelade, P.N. Pusey, Dynamic light-scattering by nonergodic media – brownian particles trapped in polyacrylamide gels, Phys. Rev. A 42 (1990) 2161–2173.

[36] W. Vanmegen, S.M. Underwood, P.N. Pusey, Nonergodicity parameters of colloidal glasses, Phys. Rev. Lett. 67 (1991) 1586–1589.

[37] J.Z. Xue, D.J. Pine, S.T. Milner, X.L. Wu, P.M. Chaikin, Nonergodicity and light-scattering from polymer gels, Phys. Rev. A 46 (1992) 6550–6563.

[38] F. Scheffold, S.E. Skipetrov, S. Romer, P. Schurtenberger, Diffusing-wave spectroscopy of nonergodic media, Phys. Rev. E 63 (2001).

[39] K.N. Pham, S.U. Egelhaaf, P.N. Pusey, W.C.K. Poon, Glasses in hard spheres with short-range attraction, Phys. Rev. E 69 (2004).

[40] W. Vanmegen, S.M. Underwood, Dynamic-light-scattering study of glasses of hard colloidal spheres, Phys. Rev. E 47 (1993) 248–261.

[41] D. El Masri, G. Brambilla, M. Pierno, G. Petekidis, A.B. Schofield, L. Berthier, L. Cipelletti, Dynamic light scattering measurements in the activated regime of dense colloidal hard spheres, J. Stat. Mech. Theory Exp. (2009) P07015.

G Model
COLSUA-19563; No. of Pages 6

ARTICLE IN PRESS

6 *G.R. Iglesias et al. / Colloids and Surfaces A: Physicochem. Eng. Aspects xxx (2014) xxx–xxx*

[42] N. Freiberger, M. Medebach, O. Glatter, Melting behavior of shear-induced crystals in dense emulsions as investigated by time-resolved light scattering, J. Phys. Chem. B 112 (2008) 12635–12643.

[43] S. Kirsch, V. Frenz, W. Schartl, E. Bartsch, H. Sillescu, Multispeckle autocorrelation spectroscopy and its application to the investigation of ultraslow dynamical processes, J. Chem. Phys. 104 (1996) 1758–1761.

[44] A.P.Y. Wong, P. Wiltzius, Dynamic light-scattering with a CCD camera, Rev. Sci. Instrum. 64 (1993) 2547–2549.

[45] L. Cipelletti, D.A. Weitz, Ultralow-angle dynamic light scattering with a charge coupled device camera based multispeckle, multitau correlator, Rev. Sci. Instrum. 70 (1999) 3214–3221.

[46] A. Knaebel, M. Bellour, J.P. Munch, V. Viasnoff, F. Lequeux, J.L. Harden, Aging behavior of laponite clay particle suspensions, Europhys. Lett. 52 (2000) 73–79.

[47] L. Cipelletti, L. Ramos, Slow dynamics in glasses, gels and foams, Curr. Opin. Colloid Interface Sci. 7 (2002) 228–234.

[48] V. Trappe, E. Pitard, L. Ramos, A. Robert, H. Bissig, L. Cipelletti, Investigation of q-dependent dynamical heterogeneity in a colloidal gel by X-ray photon correlation spectroscopy, Phys. Rev. E 76 (2007) 7.

[49] L. Cipelletti, S. Manley, R.C. Ball, D.A. Weitz, Universal aging features in the restructuring of fractal colloidal gels, Phys. Rev. Lett. 84 (2000) 2275–2278.

[50] V. Viasnoff, F. Lequeux, D.J. Pine, Multispeckle diffusing-wave spectroscopy: a tool to study slow relaxation and time-dependent dynamics, Rev. Sci. Instrum. 73 (2002) 2336–2344.

[51] L. de Campo, A. Yaghmur, L. Sagalowicz, M.E. Leser, H. Watzke, O. Glatter, Reversible phase transitions in emulsified nanostructured lipid systems, Langmuir 20 (2004) 5254–5261.

[52] A. Yaghmur, L. de Campo, L. Sagalowicz, M.E. Leser, O. Glatter, Emulsified microemulsions and oil-containing liquid crystalline phases, Langmuir 21 (2005) 569–577.

[53] M. Tomsic, F. Prossnigg, O. Glatter, A thermoreversible double gel: characterization of a methylcellulose and kappa-carrageenan mixed system in water by SAXS, DSC and rheology, J. Colloid Interface Sci. 322 (2008) 41–50.

[54] S. Guillot, M. Tomsic, L. Sagalowicz, M.E. Leser, O. Glatter, Internally self-assembled particles entrapped in thermoreversible hydrogels, J. Colloid Interface Sci. 330 (2009) 175–179.

[55] P.N. Pusey, W. Vanmegen, S.M. Underwood, P. Bartlett, R.H. Ottewill, Colloidal fluids, crystals and glasses, Physica A 176 (1991) 16–27.

[56] W. Vanmegen, P.N. Pusey, Dynamic light-scattering study of the glass-transition in a colloidal suspension, Phys. Rev. A 43 (1991) 5429–5441.

[57] D. El Masri, M. Pierno, L. Berthier, L. Cipelletti, Ageing and ultra-slow equilibration in concentrated colloidal hard spheres, J. Phys.: Condens. Matter 17 (2005) S3543–S3549.

[58] A. Duri, H. Bissig, V. Trappe, L. Cipelletti, Time-resolved-correlation measurements of temporally heterogeneous dynamics, Phys. Rev. E 72 (2005).

[59] N. Welsch, A. Wittemann, M. Ballauff, Enhanced activity of enzymes immobilized in thermoresponsive core–shell microgels, J. Phys. Chem. B 113 (2009) 16039–16045.

[60] Y. Lu, P. Spyra, Y. Mei, M. Ballauff, A. Pich, Composite hydrogels: robust carriers for catalytic nanoparticles, Macromol. Chem. Phys. 208 (2007) 254–261.